# Sedimentological and dendrochronological indicators of coastal storm risk in western France

Pierre Pouzet, Marc Robin, Armelle Decaulne, Bastien Gruchet, Mohamed Maanan

1 **Sedimentological and dendrochronological indicators of coastal storm risk in western**

2 **France**

3

4 Pouzet Pierre[1*], Robin Marc[1], Decaulne Armelle[2], Gruchet Bastien[3], Maanan Mohamed[1]

5

6 [1] Université de Nantes, LETG CNRS, Nantes, France.

7 [2] CNRS LETG, Nantes, France.

8 [3] IGARUN, Université de Nantes, France.

9 * Corresponding author. E-mail: pierre.pouzet@univ-nantes.fr

10 **Abstract**

11 This paper compares results from two different environmental methods to observe past storm

12 impacts: the back coastal barrier stratigraphical and dendrochronological archives. With a

13 detailed historical database of the past 50 years storm observations, we discuss the

14 combination of results from these two methods in a coastal study located in western France.

15 The study shows that neither tree ring nor sedimentological results build a complete storm

16 chronology by themselves. However, the combination of the two is sufficient to detect the

17 strongest storms, which caused marine flooding. Comparing them with an accurate impact of

18 storm chronology, extracted from written sources to test their robustness, we show that the

19 combination of these two approaches offer a complete dataset. From this exhaustive historical

20 sequence ranging from 1955 to 2016, three winters with major storms are highlighted in

21 Traicts du Croisic: 1990, 1978 and 1972. Combining dendrochronology and sedimentology

22 therefore enables a better understanding of extreme storm occurrences.

23

24 **Keywords:** Atlantic coast, extreme events, environmental indicators, ecological damages.

25

26 **Highlights**

27 Dendrochronology detects storm events using a tree-ring disturbance analysis.

28 Sedimentological indicators identify extreme events with marine flooding.

29 Coupling the two proxies is a powerful tool to characterize coastal extreme events.

## 1. Introduction

Documenting past storm impacts on coastal environments is a methodological challenge. This challenge must be based on the analysis of various indicators and their combination to ensure accuracy in reconstructing the extreme environmental parameters creating these disturbances. Several methods were used in scientific literature (reviews in Chaumillon et al., 2017; Goslin and Clemmensen, 2017). Many indicators, such as speleothems (e.g. Frappier et al., 2007; Zhu et al., 2017), cliff top deposits (e.g. Dewey and Ryan, 2017; Hall et al., 2006; Hansom and Hall, 2009), corral (e.g. Gardner et al., 2005; Hongo, 2018; Scoffin, 1993) and diatom (e.g. Nodine and Gaiser, 2015; Stager et al., 2017) survival or disappearance, detection of marine intrusions into a back-barrier sedimentary sequence with the buildup of washover fan (e.g. Feal-Pérez et al., 2014; Liu and Fearn, 2000; May et al., 2017; Naquin et al., 2014; Wang and Horwitz, 2007), have enabled the detection of past meteorological disturbances. Another biogeographical approach, dendrochronology, can be used to document past storms from the tree-ring disturbance it encounters during its lifespan (Schweingruber, 1996; Speer, 2012). To complete the results from the sedimentological and dendrochronological approaches, historical archives of storms were consulted, adding exhaustive and precise information on past storms (Garnier et al., 2017; Gottschalk, 1977; Hickey, 1997; Lamb and Frydendahl, 1991; Lamb, 1995).

This study seeks to highlight the combination of results from washover detection into a sedimentary sequence and a dendrochronological approach. Stratigraphy in washover context has often been used to document and date past storms (e.g. Bregy et al., 2018; Donnelly et al., 2004; Kenney et al., 2016; Liu and Fearn, 1993; Sabatier et al., 2008); in the context of violent winds, dendrochronological studies are rare. Tree-ring approaches have seldom been used in coastal environments; sea-shore erosion quantification and survey is then the main interest, analyzing exposed roots (Rovera et al., 2013), as was done along mountain torrents (Gärtner, 2007; Gärtner et al., 2001; Hitz et al., 2008), gullies (Malik, 2008) or along rivers (Begin, 1990; Begin et al., 1991). Other tree-ring approaches were used recently to reconstruct past climatic variations, mostly with chemical indicators (Berkelhammer and Stott, 2011, 2008; Brienen et al., 2012). The disturbance of tree-ring patterns to reconstruct storms is seldom in international literature: one study identified past hailstorm marks using damage made in tree trunks (Hohl et al., 2002), and few others studied records of ice storms (Lafon and Speer, 2002; Olthof et al., 2003; Travis and Meentemeyer, 1991). Here, in the absence of coastal erosion and exposed roots, we focus on tree stems and adapt the tree-ring

method previously used for geomorphic processes on slopes (e.g. Decaulne et al., 2014, 2012; Martin and Germain, 2016). Based on reports of forest damage from strong winds, tree stability may be affected in a similar way to a snow avalanche over a short period of time (Everham and Brokaw, 1996).

We focus on the storm reconstruction of the last 50 years based on these two indicators; results are compared with historical data for each of the indicators used. We then discuss the relevance of dendrochronology and sedimentology using historical proxies, and finally question the relevance of the combination of the two methods.

## 2. Study area

The western coast of France is an important storm - crossed area (Chauveau et al., 2011; Feuillet et al., 2012). The selected study site is located in the central Pays-de-la-Loire region: Traicts du Croisic and the nearby Pen Bron forested dune. This area is characterized by its high morphogenic activity coastal marsh (Fig. 1), which is separated from the sea by a sandy barrier and is ideal for detecting recent storms (Baldock et al., 2008; Pierce, 1970; Switzer and Jones, 2008; Zecchetto et al., 1997). The highest tidal ranges are from 6 to 7 meters (Service Hydrographique et Océanographique de la Marine). With protecting dunes reaching nearly 10 m asl, only storms which were concomitant to the high tide can be observed (Le Roy et al., 2015). The selected study site is exposed to western winds (from SW to NW) and marine flooding. This specific area was selected as the back barrier coastal depositional environment has been preserved from anthropogenic activities over the last 300 years, as highlighted in a GIS chronological analysis based on IGN (French National Geographic Institute) data, together with an historical and topographical study map that identified the urban evolution and landscape changes (with the method extracted from Pouzet et al., 2015). A few kilometers northward, dendrochronological analyses were also carried out from the *Pinus pinaster* forest in the Pen Bron dunes (Fig. 1). Precise coordinates of each dendrochronological and sedimentological core can be found in Table 1.


## 3. Material and methods

### 3.1. Historical data

### 3.1.1. Meteorological archives: determining storm occurrence

93   To rebuilt a chronology of storms that have crossed the study area, historical documents were
94   consulted: (i) documents from libraries and archives, (ii) narrative sources (chronicles, diaries,
95   memoires etc.), and (iii) old maps. These documents contain observational and descriptive
96   data on past extreme weather occurrences, useful to estimate the intensity of each recent
97   event. However, before being used to reconstruct the storms and sea flooding chronology over
98   the last seven decades, this data was analyzed and evaluated. The reliability of a written
99   document is evaluable on the basis of (i) the witness statement by the author and (ii) the
100  institutional framework of the evidence record (Athimon et al., 2016; Athimon and Maanan,
101  2018, submitted). Moreover, it was necessary to inspect testimonies with several sources. The
102  aim was to have a more precise and exhaustive record of each event within a precise temporal
103  and spatial frame.

104  We also considered records from instrumental installations such as meteorological data
105  collected by Meteo France for the period (within the study area). On the Meteo France storm
106  report website *http://tempetes.meteofrance.fr/*, numerous details about recent storms are
107  available. However, this data is limited: the website provides accurate information about well-
108  known storms only. Therefore, storms that have severely impacted the country, but that were
109  not significant at a regional scale, are not documented there. Thus, we had to consult more
110  accurate sources, such as local archives. The detailed historical investigation, bearing in mind
111  the reliability of all documents, is needed in combination with other digital sources to obtain
112  the most accurate chronology possible.

113  **3.1.2. Reanalysis data to accurately reconstruct recent wind conditions**

114  The HOMERE © database was analyzed (Boudiere et al., 2013) using the WAVEMATCH III
115  (v. 4.09) model. This reanalysis enabled the reconstruction of windy conditions over recent
116  years, complementing the wind data extracted from weather database (Meteo France). After
117  selecting a mesh located a hundred meters offshore of the study area, we extracted all wind
118  and wave data with MATLAB ©. The database provides hourly mean wind direction and
119  speeds for the 1994 – 2012 period, calculated from uwnd (eastward wind) and vwnd
120  (northward wind) raw data. It was used to statistically detect the windiest years, and to note
121  the years where the most south-western winds were observed as standing trees are mostly
122  tilted by south-western winds, and to extract the years where the highest number of hourly
123  devastating winds are modeled.

124  **3.2. Sedimentological record of storms**

125  Extracting cores from Traicts du Croisic back barrier coastal marsh, as close as possible to the

126  Pen Bron dune barrier, offers a sedimentological record of the coastal marshs' recent

127  development (Pouzet et al., 2018, submitted). The morphology of lacustrine sediment layers

128  differs from the ones received from marine conditions, seen as allochthonous layers within the

129  cores (Baumann et al., 2017; Chaumillon et al., 2017; Das et al., 2013; Liu, 2004; Orme et al.,

130  2015; Sabatier et al., 2010, 2008). A method enabling the characterization of sediment

131  parameters was set. Three sediment cores,  50 mm in diameter and a maximum of 100 cm

132  long were extracted with an Eijkelkamp © gravity corer in August 2016; the position of each

133  core was localized with a Trimble Differential Global Positioning System (DGPS). All

134  locations were tied to IGN benchmarks and levelled with respect to the NGF datum. Cores

135  were first longitudinally sliced, photographed and described. Then, the Avaatech© XRF core

136  scanner was used to carry out high-resolution elemental analyses of the split sediment cores.

137  Element intensities, normalized by the total intensity (count per second of each spectrum:

138  cps); and element ratios were calculated (Bouchard et al., 2011; Chagué-Goff, 2010; Martin et

139  al., 2014; Sabatier et al., 2012). The Scopix© system was used to take X radiographs to

140  precisely describe  the sedimentology of the three cores (Migeon et al., 1998), commonly

141  used to identify finer washovers, shells or pebbles within the invisible part of the core into

142  several studies (e.g. Coor et al., 2009; Sabatier et al., 2012; Scott et al., 2003). Colorimetric

143  analyses estimated the lightness of sediments with a Minolta© Cm-2600d spectrometer

144  (Debret et al., 2011; Polonia et al., 2013) as Mix et al., 1995 demonstrated a positive

145  correlation between lightness and carbonate content. A MS2E-1© Bartington-type measured

146  the magnetic susceptibility (MS) of each centimeter for a magnetic oxide and clay detection

147  (Bloemendal and deMenocal, 1989; Wassmer et al., 2010), a proxy previously used with

148  success in some paleoclimatic studies (e.g. Begét et al., 1990; Buynevich et al., 2011; Roy et

149  al., 2010). For a grain size analysis (mean grain size : MGS), the main proxy used in most of

150  storminess reconstructions (e.g. Chaumillon et al., 2017; Eden and Page, 1998; Liu and Fearn,

151  1993; Noren et al., 2002), measured by a Malvern Mastersizer 2000© laser beam grain sizer

152  (Parsons, 1998; Yu et al., 2009), sediment cores were sampled every 1 cm, and every 0.5 cm

153  for dating.

154  Once layers are characterized as marine, dating them is essential, in order to associate them

155  with stormy conditions in the second step. Dating was established from a combination of two

156  short-lived radionuclides: lead ($^{210}$Pb)  and cesium ($^{137}$Cs) isotopes (Hippensteel and Martin,

157  1999; Lima et al., 2005; Sabatier et al., 2008). The first is a naturally-occurring radionuclide

158  rapidly incorporated into the sediment from water column scavenging and atmospheric fallout

159  ($T_{1/2}$ = 22.3 years). $^{137}$Cs ($T_{1/2}$ = 30 years) is an artificial radionuclide related to the

160  atmospheric nuclear weapons tests in the early sixties (maximum near 1963 in the northern

161  hemisphere) and to the Chernobyl accident in April 1986. Activities of $^{210}$Pb and $^{137}$Cs were

162  determined at the University of Bordeaux on 3-4 g of dried sediment by gamma spectrometry,

163  using a well-type, high efficiency low background γ detector equipped with a Cryo-cycle

164  CANBERRA © (Pouzet et al., 2018, submitted).

**3.3. Dendrochronology**

166  In order to find the most appropriates trees, we first used reanalysis data to identify the areas

167  with the highest winds (Fig. 2). During the 1994 – 2012 period, the wind direction was mainly

168  from south and south west, with the strongest mean wind from the south west. This area is

169  dominated by high south-westerly winds, corresponding with the visual observations made in

170  the field, as most of disturbed trees are inclined in an SW-NE axis. From a historical map

171  study, we then identified the location of the oldest trees in the area. In the selected site, we

172  finally identified selected seventeen trees to core, including a high proportion of SW-NE

173  disturbed trees.

174  Trees exposed to high winds develop specific tree-ring patterns (Schweingruber, 1996), as

175  they do when impacted by other geomorphic processes: stormy years show a significantly

176  wider tree-ring expressed as compression wood as the species investigated here is mostly

177  composed of *Pinus pinaster* (Fig. 3B).

178  To identify the stormy years during the lifespan of the trees, twenty disturbed *Pinus pinasters*

179  were sampled with a Mattson© corer following classical dendrochronological methods

180  (Grissino-Mayer, 2003). Trees presenting tilting and located at the fringe, closer to the sea

181  were selected and sampled at breast height. A standard Global Positioning System (GPS) was

182  used to precisely position the selected trees. Sampling was made throughout the entire

183  thickness of the trunk, in the disturbance direction (mostly from south-west, see Table 1) to

184  encompass the axes where the largest dissymmetry is expected (full expression of

185  compression wood). Following dendrochronological preparation guidelines (Speer, 2012),

186  samples are dried at room temperature over two weeks inside the protective plastic pipes they

187  were placed in at the sampling stage; then samples are mounted on wood supports and sanded.

188  A fresh scalpel cut was also done before measuring ring widths on the Lintab Rinntech©

6

189   platform at LETG laboratory. TsapWin© software enabled measurements and gave a precise
190   chronology of all tree sampled.

191   To fit the tree growth pattern, we considered successive vegetative and dormancy seasons as
192   one year, i.e. March to October as the vegetative season, and November to February as the
193   dormancy season. Any disturbance (e.g. tilting during an excessive wind event) experienced
194   by a tree during its dormancy phase will be visible within the formation of the next tree ring
195   during the following vegetative season : during the vegetative season, the tree-ring cells will
196   organize to counterbalance the stress from the dormancy period, i.e. by producing
197   compression wood, visible through an asymmetric growth (cells produced on the face
198   exposed to the stress will be smaller than those on the opposite face, which will be much
199   larger than during a normal growth). A complete tree season, called "tree year", is from
200   November of the calendar year n-1 to October of the calendar year n.

201   To detect wind disturbance axes, a precise comparison is made between tree-ring widths
202   (TRW) of asymmetric radiuses C and D of all trees sampled (Fig. 3C). Before extracting
203   growth disturbances and identifying years with increasing growth values in C, concomitant to
204   a decrease in growth values in D visually, we first have to calculate an evolution rate between
205   each tree year mathematically as follows:

206   $$GE = (TRW_n - TRW_{n-1}) / TRW_{n-1} * 100$$

207   *Where GE is the growth evolution, $TRW_n$ is the tree-ring width at year n and $TRW_{n-1}$ is tree-*
208   *ring width at year n-1.*

209   From a double visual and mathematical analysis, a disturbed year that experienced stress is
210   considered when:

211   - The width of the tree-ring decreases in C by at least -25% from the previous year value,
212   together with an increase of D radius (GE of C radius < -25, and GE of D radius > 0);

213   - The width of the tree ring increases in D radius by at least +25% from the previous year
214   value, together with a decrease of the C radius (GE of D radius > 25, and GE of C radius < 0).

215   In cases of successive disturbed years, only the first year of disturbance is taken into account
216   as the tree might react to a disturbance for several years (Schweingruber, 1996). A year is
217   recognized as significant if at least two trees react, in a minimum of five living trees (25% of
218   the number of trees sampled) i.e. from 1955. These criteria set the dendrochronological
219   chronology into a temporal scale starting in November 1955 and ending at the last vegetative

7

year of the samples, i.e. October 2016. For each year of the chronology, an index of storm disturbance (ISD) is calculated to estimate the impact of one storm or a series of storms during a year, as follows:

$$ISDn = (DTn*100)/LTn$$

*Where ISDn (as a percentage) is the Index of Storm Disturbance of the year n, DTn is the number of disturbed trees during the year n and LTn is the number of living trees during the year n.*

## 4. Results

### 4.1. Marine occurrences from sedimentological archives

#### 4.1.1. Dating of Traicts du Croisic sequences

[210]Pb profile of Traicts du Croisic (TC) core is classic, with decreasing activity reaching negligible levels below 20 cm (Fig. 4). A mean sediment accumulation rate of 0.24 cm yr^{-1} was estimated, used to extrapolate ages by assuming that the mean sedimentation rate was constant for horizons beyond the timescale covered by [210]Pb. The sedimentary ^{137}Cs profile helped to estimate that the ^{210}Pb chronology ranges from 1916 AD (Anno Domini) ± 13 years to 2016 AD: [137]Cs activities disappear below the deep "nuclear weapons tests" peak at about 12-13 cm, in 1963 according to ^{210}Pb dating. The 1986 Chernobyl accident can also be estimated with a small rebound of the ^{137}Cs curve at 7 cm depth from ^{210}Pb dating (Lomenick and Tamura, 1965; Ritchie and McHenry, 1990; Walling and He, 1999). To fit the dendrochronological chronology, which goes no further than 1955 AD ± 8 years, the sedimentological dating assessment goes no further than 15 cm depth in this study.

#### 4.1.2 Allochthonous marine layers detection

Cores, drilled in a coastal back barrier environment, present an original clayey-silty context, with small grain sizes, low values of lightness and a high magnetic susceptibility. Terrestrial elements such as Iron (Fe) or Titanium (Ti) are significantly more dominant than marine elements (Strontium: Sr or Calcium: Ca). Consequently, in a back barrier type sequence, low ratios of Sr/Fe and Ca/Ti must be identified. A marine intrusion into this environmental condition must leave evidence such as high values of mean grain size (with sands), geochemical ratios, lightness and a low magnetic susceptibility (Chagué-Goff et al., 2017;

Coor et al., 2009; Lu and An, 1998; Mix et al., 1995; Peng et al., 2005; Roy et al., 2010). The post-1955 layers are encompassed within the upper 15 centimeters of the three cores (Fig. 4).

We reported in core TC1 a unique marine intrusion at 9 cm depth with a high increase of MGS passing from 110μm to 180μm, two geochemical increases from 0.1 to 0.2 Sr/Fe and 8 to 20 Ca/Ti, a (high starting of lightness increase) and a state of neutral to low MS. The Scopix image also shows the coarse sandy incursion. Dating assesses this layer to be 1977 AD ± 3 years. A second marine incursion hypothesis was rejected at 11 cm depth because geochemical indicators are stable despite a high MGS increase, rendering the marine origin of these sediments uncertain. In TC2, one incursion is also reported at nearly 11 cm depth for a storm in 1972 AD ± 4 years. This layer marks the beginning of a high increase of MGS (from 20 to 90μm), and a slight Sr/Fe increase from 0.2 to 0.3, an increase of lightness and a hollow in the MS curve. In TC3 core, sediments are less sorted, and a high variation in MGS is observed. Two certain marine intrusions are extracted at 6 and 11 cm depth, dated as 1990 AD ± 2 year and 1972 ± 4 years. The first layer shows a high MGS, Sr/Fe, and lightness increases respectively from 50 to 270μm, 0.05 to 0.1 and 47% to 48% with a low MS level. The second layer is identified at 11 cm depth: despite high MGS starting within the upper unit, the accurate geochemical and Scopix proxies respond with a double Sr/Fe and Ca/Ti low increase, and a fall of MS. We identify clearly in the Scopix image a *Venerupis decussata* shell, typical of a marine environment. At 13 cm depth, we observed a high MGS increase, which probably do not correspond to a marine occurrence as all other proxies do not follow MGS.

**4.1.3 Correlation of stormy sedimentological signatures with historical written records**

From the analyses of sediments retrieved from the back barrier coastal marsh area, three main post-1955 dates point out potential overwashs in 1972, 1977 and 1990. Historical records show all three dates correspond either to one strong storm event (February 13, 1972) or to a series of storms (December 2, 1976 and January 11, 1978; January 25, 1990 February 2, 1990 and February 26, 1990) crossing the area during the winter, causing severe damage. During the three recorded events a high tide coefficient was recorded, contributing to the deposition of the marine layer observed.

During the February 13, 1972 storm, maximum wind speed was recorded up to 172 km/h in western France; damage included uprooted trees, broken steeples, toppled cranes, destroyed dikes, damage to boats and roofs (http://tempetes.meteofrance.fr/Tempete-du-13-fevrier-

9

1972.html; Municipal Archives, Nantes, 1038 W 327; Departmental Archives of Vendée, 78/31 1953-1975 – tempête du 13 février 1972). Starting on the 13 December of 1972, it mostly hit western France over three days, with a tide coefficient of 75 to 100 at Le Pouliguen harbor, located two kilometers south of Traicts du Croizic (according to the Service Hydrographique et Océanographique de la Marine). Many coastal floods and nearly 30 deaths and fatalities were recorded.

The second date derived from the sedimentological analyses is 1977. From historical archives, two different events correspond: December 2, 1976 and January 11, 1978. In the first case the tide coefficient was very low, ca. 50; in the second event it reached 109 (SHOM). The second date is therefore more likely. With ten deaths and fatalities reported, the early 1978 storm crossed a large part of the country as damage was reported from Dunkirk (500 kilometers northward) to the Gironde estuary (200 kilometers southward), with numerous shipwrecks and marine flooding (Le Marin 1595, MetMar 101). During the same storm *"numerous houses have been blown away by sea waves"* and several storm surges were reported in eastern England, where the storm was much more mediatized and wind records reached more than 130 km/h (Steers et al., 1979). While historical sources mentioned uprooted trees and devastated buildings in many parts of the country, no maximal wind speed is documented in France.

Finally, in 1990, three different storms crossed the study area causing widespread damage, including a high tide coefficient: in February 26-28, 1990, a 104 tide coefficient (SHOM) was recorded. The successive storms caused 100 fatalities over the whole country, with winds reaching 176 km/h maximum in western France; many flooded houses and broken dikes were reported (http://tempetes.meteofrance.fr/Daria-le-25-janvier-1990.html, http://tempetes.meteo france.fr/ Herta-le-03-fevrier-1990.html, and http://tempetes.meteofrance.fr/Viviane-du-26-au-28-fevrier-1990.html; Municipal Archives of Nantes, 23 Z 355; 24 PRES 152, 05/02/1990 and 24 PRES 152, 27 and 28/02/1990; Departmental Archives of Vendee, 1856 W 38).

**4.2. Storm detection using dendrochronology**

**4.2.1 Tree Ring Width analysis**

From the twenty trees sampled, seventeen present readable cores enabling the creation of a robust chronology. On the three eliminated cores, the latewood boundary and the next earlywood were not clearly separated, possibly due to the lack of harsh winter at the study site, which benefits from a pronounced temperate maritime climate. The TRW analysis

highlights a number of years with wood reaction formation (Fig. 3C). Several years were disregarded as they concern only one tree (Fig.6). From this chronology, the temporal distribution of growth disturbances, i.e. the onset of growth eccentricity (corresponding to the unequal growth of the tree along the main axis C-D, i.e. tilting of the tree), and strong growth disturbances in relation to the stated criteria is revealed (Fig. 5). Numerous tree years have been disturbed since 1955. Depending on their location within the stand, trees show a high variation of the response-year occurrence. For example, tree PB05 is located on the SW-NE edge of the stand (Fig. 1) and shows 13 response years over the 61 year period, providing a return period of impacts due to storms of 4.7 years. On the other hand, sample PB10, which was less exposed and located further inside the stand with a S-N orientation (Table 1, Fig. 1), recorded only one major disturbance at the sampling height. On the whole, the most exposed trees to southwestern, south-southwestern or west-southwestern high winds located at the edge of the stand are the most exposed, as shown by the strongly impacted samples. This observation is in accordance with the main trajectories of extratropical storms, coming from a south-western direction in southern France and from a western direction in north-west France (Lozano et al., 2004); in the study area, the highest winds mainly come from a SW direction (Fig. 2). Over the 61 years covered by dendrochronology, 19 years present strong evidence of growth disturbance in at least two trees. According to these results, a mean return period of strong winds, or storms, is assessed to be 15.6 years at the study site (Fig. 5).

With an ISD of 33%, the 1965 tree year (from November 1964 to October 1965) is the most impacted, with only 6 trees alive at this time (Fig. 5, Fig. 6). Another significantly impacted tree year is 1998, with nearly 30% of the 17 pines sampled showing clear signs of responses according to the identification criteria. Those showing more than 20%, 1977 (12 living trees), 2002, 2007 and 2014 (17 living trees) are also strongly impacted. 2009, 2013 (17 living trees) and 1978 (13 living trees) are considered as significant stormy years too. Other years with a lesser impact on trees are 1983, 1986, 1987, 1989, 1990, 1996, 2004, 2006, 2012 and 2016,. Several years were disregarded as they did not fulfill the established criteria. Finally, since 1955, data shows that as much as 83% of storms recorded in the chronology derived from tree-ring analyses occurred during the three winter months (December, January and February).

**4.2.2 Correlation of dendrochronological results with historical data**

*4.2.2.1 A clear correlation between tree disturbances and storm occurrence*

Dendrochronological results were compared with written storm records (Table 2). A clear correlation can be observed between impacted tree years and storm occurrences in the study area. Correlations were considered positive if an historical stormy year (year with at least one reliable historical storm record) corresponds to an impacted tree year, as described in the dendrochronological method. First of all, we observed that each impact tree year is correlated with at least one known storm passing through the study area, except in 2002. On the whole, during the 61 years of the dendrochronological study, 50 years (80%) show a good correlation with storm records. We also reported six years (10%) of uncertainties due to a lack of precise recorded information about the wind impacts reported in the study area. The six other tree years show no correlation between dendrochronological results and storm reports: 1967, 1972, 1980, 1999 and 2000 are not revealed within the tree-ring patterns even though impacting storms were reported, and 2002 shows tree-ring patterns when no storm was reported.

Tree-ring results are compared with reanalysis data. The highest winds observed for eleven of the twelve years from 1994– 2012 (Table 2) correspond to storm records (Fig. 7). 2007 is the only year with high wind records not correlated to any storm. The main wind direction during these extreme records is SW-NE; which is also the main direction of tilting in trees sampled in the study area. Therefore, we consider it highly probable that growth disturbances observed in the trees sampled were produced by storms during the period 1994-2012. From these positive results, we can extrapolate that earlier growth-disturbance signals are also due to storm occurrences. We consider dendrochronology a good proxy to reveal past storm occurrences.

*4.2.2.2 Understanding absences of correlations*

Reanalysis data was also used to understand the apparent absence of correlation between the tree-ring analyses and historical data of storm occurrences. The annual study of wind speed and direction (Fig. 8) and the study of the highest wind speed records (Fig. 9A and B) over the period 1994-2012 are combined with Meteo France data available for the period 1955-2016.

Tree-ring data reveal growth disturbances in 2001-2002 when no storm was recorded (Fig. 6, Table 2). Reanalysis data shows that this growth disturbance follows two years of strong winds (Fig. 8). Years 2001 and 2002 were the two windiest years without storms, with an annual mean wind speed of almost 20.5 to 21 km/h. Years 1998 and 2012 were very windy

also, recording high wind speeds and storms (Fig. 7, Fig. 9A and B), influencing the annual wind speed average. Altogether, the cumulative winds in 2001 and 2002, with a prevailing SW wind, may have impacted the trees and contributed to their tilting, creating a durable growth disturbance that also extended over the 2002 tree ring.

Another type of non-correlation appeared during the years 1999 and 2000: despite a series of impacting storms (especially in 2000), no major disturbances appear in tree-ring patterns (Fig. 6, Table 2). These well documented events, including the Lothar and Martin severe storms are highlighted too in the reanalysis data: high values of extreme winds were oriented to be recorded in the study area (Fig. 7, Fig. 9B). In the winter of 1998, high annual mean wind speeds (Fig. 8) with intense and extreme wind speeds were encountered (Fig. 9A and B). Three devastating storms crossed the study area in 1998 (Table 2). The year 1998 is clearly recorded in the tree-ring patterns; the following years 1999 and 2000 might not have recorded the disturbances as tree-ring development was still suffering from the 1998 impacts that lasted over a few growth seasons, as described by Schweingruber (1996).

Three more years, 1967, 1972 and 1980, do not show correlations between tree-rings and written sources (Fig. 6, Table 2). The timing of these stormy seasons does not fit with the period covered by the reanalysis data. However, Meteo France storm database enabled the extraction of the maximum wind speed record maps (Fig. 10) for each known storm (http://tempetes.meteo.fr/Tempete-du-12-mars-1967.html,           http://tempetes.meteofrance.fr/ Tempete-du-13-fevrier-1972.html,       http://tempetes.meteo.fr/Tempete-du-15-decembre1979. html). The storms of February 13, 1972 and December 15, 1979 present maximum instant wind from NW to SE; this is the opposite to the core extraction from trees, oriented SW-NE: these storms have not left disturbances in the core extracted, therefore are invisible from the dendrochronological approach. Regarding the March 13, 1967 event, its orientation was mainly W-E; despite the limited information available regarding this storm, only one tree showed changes. However, only a few of the tree samples go back to this period, and those living then were young and therefore more flexible and wind resistant.


## 5. Discussion: What is the value of combining sedimentological and dendrochronological results?

Independently, sedimentological and dendrochronological methods exhibit the dating of some very destructive storms and their impacts on a back barrier coastal marsh and on trees, in a

13

specified area. The sedimentological study shows some of the strongest marine flooding reported in Traicts du Croisic, and the tree-ring analysis offers an overview of the occurrence of the windiest storms at a forest scale. A high wind storm crossing at low tide or during a low tide coefficient day will not be recorded in the sedimentological archives but can be found in tree-ring patterns (this can be questioned for the 1998 stormy year). Conversely, a small depression crossing at a maximum tide coefficient during high tide with light winds reported can produce washover without creating major disturbances in tree-ring patterns, and this is one of the last remaining questions for the 1972 hypothesis. The crossing of a storm producing very high winds and widespread marine flooding may be the only hypothetical correspondence between the two methods, as this study shows for the 1990 events.

This study shows that this precise scenario may have only appeared three times during the last 61 years. The winter of 1989-90 data showed a major disturbed season from both proxies, and in meteorological archives. With more uncertainties in the sedimentological and meteorological sources, 1978 is also interpreted as a storm-year in both proxies. However, the possible confusion regarding the precise sedimentological year crossing two possible storms (December 1976 and January 1978), and the lack of wind speed details do not enable a clear interpretation. In 1972, the combination of proxies is not robust either: significant marine flooding is found in numerous cores; the dendrochronological signature is lacking as this storm caused mainly northwesterly high winds, i.e. perpendicular to the cores extracted from trees. Historical sources reveal that the 1972 event was very destructive. Data from the two methods complement one another by identifying different types of impacts from an extreme wind event.

The availability of valid historical data remains crucial, enabling the understanding of events extracted from tree-ring analyses. The main limit in tree-ring research is its potential destructive impact: in order to avoid felling most of the trees on the back dune, only cores are extracted from trees depending on the direction of their tilt, which reflects the most accurate impact of the winds on the trees. The observation of these cores does not reveal events originating out of the main tilting direction, which might have had a strong impact on tree-ring patterns. Although most of strongest storm winds of the study area come from the SW, some storms hit the area from another direction, as during the 1972 event. This event is invisible without a full view of the tree-ring patterns on the trunks, i.e. invisible without sawing the trees or multiplying the orientations of cores through the trunks. The dendrological process-event-response analysis associated to index values, elaborated from Shroder, 1980

and Shroder, 1978 is robust; however, the time lapse for recovery after a geomorphic impact (here occasional severe winds) is unknown. As for caution, we used the first year of occurrence of tree-ring disturbance, letting the following years in the shadow, unsure of the ability of the tree to reveal successive event. The more common use of dendrochronology in coastal environments to document severe winds is needed to refine the method and better understand the behavior of tree rings under such a forcing. From detailed meteorological data such as wind direction or intensity, we were able to confirm the dendrochronological findings, as tree-ring analysis is an accurate biological dating (Speer, 2012). The TRW variation is calculated with precise measurements and consequently exposes robust results. Concerning the sedimentological method, it is considered as fully reliable as the typical event layer is composed of texturally different sediments contrasting to the usual deposits of the sedimentation area (Chaumillon et al., 2017). Comparing to the TRW method, sedimentological dating is exposed to a lower accuracy (Binford, 1990). To build an accurate comparison with the tree-ring dating, only the more precise part of the core (the fifteen upper centimeters in this study corresponding to the stand lifespan) is analyzed. Dates found in this section reached a maximum uncertainty of four year, the crossing of washovers observed with historical data is precise enough to set solid storm hypotheses. We nowadays need other recent back barrier stratigraphical studies to compare washovers found in the Traicts du Croisic with other western France lagoonal sequences. Recent study cases of storm deposits are missing in the area; we can't compare today these sedimentological analyses with other identical setting areas nearby. However, historical data are also used here to confirm if coarse sand layers observed within the sedimentological cores were linked to the crossing of high tide coefficients and strong winds. Throughout their storm damage details, they documented breaches and marine flooding reported elsewhere in and around the vicinity of the study area. They can assure that dendrochronological and sedimentological hypotheses are reliable in spite of disadvantages described in this section.

Despite these slight limitations, both methods are efficient in their own way, and their combination helps the understanding of storm impact distribution in a specific area. The results emphasize that tree-rings can be used as a proxy to reveal severe wind conditions due to storms; however, the temporal and spatial resolution of the results is limited to the spatial distribution of trees and to their lifespan. The crossing of ancient geographical documents such as old map and aerial photography is needed to sample a relevant stand. Sedimentological archives extracted from stratigraphic cores are also relevant, showing a

good correlation with historical written sources where well-known marine flooding events are recorded. As a perspective, tree rings and sediment archives can be used as indicators regarding the environmental vulnerability to storm hazard, depending on the dimensions of the protecting dune, the presence and type of vegetation on the dune, the orientation of the coastline and more generally on the sedimentary dynamics of each area.

## 6. Conclusion

This paper shows that multi-proxies analyses are necessary to collect sufficient information to characterize coastal storms and their potential impacts. The methods, sedimentology and dendrochronology, complement the historical archives by attesting their reliability at a specific location. Sedimentology and dendrochronology have respective methodological and analytical limitations, (restraining a rigorous crossing for the construction of a coupled and unique storm chronology). The dendrochronological approach can be improved by multiplying the orientation of cores (or analyzing discs, supposing that several trees are felled). However, both are effective in detecting major recent storms in the study area using distinct environmental parameters. Sedimentology applied at a distance from the sea detects extreme wind events causing inland marine flooding, while dendrochronology detects major storms if they do not occur in successive years, due to the disturbance of tree-ring patterns that can last for several years. Both methods are thus effective in recording storm events.

The combination of the two methods clearly highlights three years, i.e. severe storms in 1990, 1978 and 1972. The results clearly show that or most known storm events recorded are recognized from the natural proxies investigated. Dendrochronology and sedimentology can thus be used together, or separately, as reliable approaches to understand the main meteorological parameters of past storms in the absence of written sources.

## 7. Aknowledgments

## 8. References

Athimon, E., Maanan, M., 2018. Severe storm, coastal flood damage, adaptation and resilience of societies during the Little Ice Age (West of France). Prog. Hum. Geogr. Submitted.

Athimon, E., Maanan, M., Sauzeau, T., Sarrazin, J.-L., 2016. Vulnérabilité et adaptation des sociétés littorales aux aléas météo-marins entre Guérande et l'île de Ré, France (XIVe - XVIIIe siècle). VertigO - Rev. Électronique En Sci. Environ. https://doi.org/10.4000/vertigo.17927

Baldock, T.E., Weir, F., Hughes, M.G., 2008. Morphodynamic evolution of a coastal lagoon entrance during swash overwash. Geomorphology 95, 398–411. https://doi.org/10.1016/j.geomorph.2007.07.001

Baumann, J., Chaumillon, E., Schneider, J.-L., Jorissen, F., Sauriau, P.-G., Richard, P., Bonnin, J., Schmidt, S., 2017. Contrasting sediment records of marine submersion events related to wave exposure, Southwest France. Sediment. Geol. 353, 158–170. https://doi.org/10.1016/j.sedgeo.2017.03.009

Begét, J.E., Stone, D.B., Hawkins, D.B., 1990. Paleoclimatic forcing of magnetic susceptibility variations in Alaskan loess during the late Quaternary. Geology 18, 40–43. https://doi.org/10.1130/0091-7613(1990)018<0040:PFOMSV>2.3.CO;2

Begin, Y., 1990. The Effects of Shoreline Transgression on Woody Plants, Upper St. Lawrence Estuary, Quebec. J. Coast. Res. 6.

Begin, Y., Langlais, D., Cournoyer, L., 1991. A Dendrogeomorphic Estimate of Shore Erosion, Upper St. Lawrence Estuary, Quebec. J. Coast. Res. 7.

Berkelhammer, M., Stott, L., 2011. Correction to "Recent and dramatic changes in Pacific storm trajectories as recorded in the δ18O of Bristlecone Pine tree ring cellulose." Geochem. Geophys. Geosystems 12, Q09002. https://doi.org/10.1029/2011GC003765

Berkelhammer, M.B., Stott, L.D., 2008. Recent and dramatic changes in Pacific storm trajectories recorded in δ18O from Bristlecone Pine tree ring cellulose. Geochem. Geophys. Geosystems 9, Q04008. https://doi.org/10.1029/2007GC001803

Binford, M.W., 1990. Calculation and uncertainty analysis of 210Pb dates for PIRLA project lake sediment cores. J. Paleolimnol. 3, 253–267. https://doi.org/10.1007/BF00219461

Bloemendal, J., deMenocal, P., 1989. Evidence for a change in the periodicity of tropical climate cycles at 2.4 Myr from whole-core magnetic susceptibility measurements. Nature 342, 897–900. https://doi.org/10.1038/342897a0

Bouchard, F., Francus, P., Pienitz, R., Laurion, I., 2011. Sedimentology and geochemistry of thermokarst ponds in discontinuous permafrost, subarctic Quebec, Canada. J. Geophys. Res. Biogeosciences 116, G00M04. https://doi.org/10.1029/2011JG001675

Boudiere, E., Maisondieu, C., Ardhuin, F., Accensi, M., Pineau-Guillou, L., Lepesqueur, J., 2013. A suitable metocean hindcast database for the design of Marine energy converters. Int. J. Mar. Energy 3–4. https://doi.org/10.1016/j.ijome.2013.11.010

Bregy, J.C., Wallace, D.J., Minzoni, R.T., Cruz, V.J., 2018. 2500-year paleotempestological record of intense storms for the northern Gulf of Mexico, United States. Mar. Geol., Geological Records of Extreme Wave Events 396, 26–42. https://doi.org/10.1016/j.margeo.2017.09.009

Brienen, R.J.W., Helle, G., Pons, T.L., Guyot, J.-L., Gloor, M., 2012. Oxygen isotopes in tree rings are a good proxy for Amazon precipitation and El Niño-Southern Oscillation variability. Proc. Natl. Acad. Sci. 109, 16957–16962. https://doi.org/10.1073/pnas.1205977109

Buynevich, I., Klein, A., FitzGerald, D., Cleary, W., Hein, C., Veiga, F., Angulo, R., Asp, N., Petermann, R., 2011. Geological legacy of storm erosion along a high-energy indented coastline: northern Santa Catarina, Brazil. J. Coast. Res. 1840–1844.

Chagué-Goff, C., 2010. Chemical signatures of palaeotsunamis: A forgotten proxy? Mar. Geol. 271, 67–71. https://doi.org/10.1016/j.margeo.2010.01.010

Chagué-Goff, C., Szczuciński, W., Shinozaki, T., 2017. Applications of geochemistry in tsunami research: A review. Earth-Sci. Rev. 165, 203–244. https://doi.org/10.1016/j.earscirev.2016.12.003

17

558 Chaumillon, E., Bertin, X., Fortunato, A.B., Bajo, M., Schneider, J.-L., Dezileau, L., Walsh, J.P.,
559     Michelot, A., Chauveau, E., Créach, A., Hénaff, A., Sauzeau, T., Waeles, B., Gervais, B., Jan, G.,
560     Baumann, J., Breilh, J.-F., Pedreros, R., 2017. Storm-induced marine flooding: Lessons from a
561     multidisciplinary approach. Earth-Sci. Rev. 165, 151–184.
562     https://doi.org/10.1016/j.earscirev.2016.12.005

563 Chauveau, E., Chadenas, C., Comentale, B., Pottier, P., Blanlœil, A., Feuillet, T., Mercier, D., Pourinet,
564     L., Rollo, N., Tillier, I., Trouillet, B., 2011. Xynthia : leçons d'une catastrophe. Cybergeo Eur. J.
565     Geogr. https://doi.org/10.4000/cybergeo.23763

566 Coor, J.L., Donoghue, J., Wang, Y., Das, O., Kish, S., Elsner, J., Hu, X.B., Niedoroda, A.W., Ye, M., 2009.
567     Development of a Long-Term Storm History for the Northwest Florida Coast Using Multiple
568     Proxies. AGU Fall Meet. Abstr. 11.

569 Das, O., Wang, Y., Donoghue, J., Xu, X., Coor, J., Elsner, J., Xu, Y., 2013. Reconstruction of paleostorms
570     and paleoenvironment using geochemical proxies archived in the sediments of two coastal
571     lakes in northwest Florida. Quat. Sci. Rev. 68, 142–153.
572     https://doi.org/10.1016/j.quascirev.2013.02.014

573 Debret, M., Sebag, D., Desmet, M., Balsam, W., Copard, Y., Mourier, B., Susperrigui, A.-S., Arnaud, F.,
574     Bentaleb, I., Chapron, E., Lallier-Vergès, E., Winiarski, T., 2011. Spectrocolorimetric
575     interpretation of sedimentary dynamics: The new "Q7/4 diagram." Earth-Sci. Rev. 109, 1–19.
576     https://doi.org/10.1016/j.earscirev.2011.07.002

577 Decaulne, A., Eggertsson, Ó., Laute, K., Beylich, A.A., 2014. A 100-year extreme snow-avalanche
578     record based on tree-ring research in upper Bødalen, inner Nordfjord, western Norway.
579     Geomorphology, SEDIMENT FLUX AND SEDIMENT BUDGET STUDIES IN COLD
580     ENVIRONMENTS:NEW APPROACHES AND TECHNIQUES 218, 3–15.
581     https://doi.org/10.1016/j.geomorph.2013.12.036

582 Decaulne, A., Eggertsson, Ó., Sæmundsson, Þ., 2012. A first dendrogeomorphologic approach of
583     snow avalanche magnitude–frequency in Northern Iceland. Geomorphology, Sedimentary
584     fluxes and budgets in natural and anthropogenically modified landscapes – Effects of climate
585     change and land-use change on geomorphic processes 167–168, 35–44.
586     https://doi.org/10.1016/j.geomorph.2011.11.017

587 Dewey, J.F., Ryan, P.D., 2017. Storm, rogue wave, or tsunami origin for megaclast deposits in western
588     Ireland and North Island, New Zealand? Proc. Natl. Acad. Sci. 114, E10639–E10647.
589     https://doi.org/10.1073/pnas.1713233114

590 Donnelly, J.P., Butler, J., Roll, S., Wengren, M., Webb, T., 2004. A backbarrier overwash record of
591     intense storms from Brigantine, New Jersey. Mar. Geol., Storms and their significance in
592     coastal morpho-sedimentary dynamics 210, 107–121.
593     https://doi.org/10.1016/j.margeo.2004.05.005

594 Eden, D.N., Page, M.J., 1998. Palaeoclimatic implications of a storm erosion record from late
595     Holocene lake sediments, North Island, New Zealand. Palaeogeogr. Palaeoclimatol.
596     Palaeoecol. 139, 37–58. https://doi.org/10.1016/S0031-0182(97)00136-3

597 Everham, E.M., Brokaw, N.V.L., 1996. Forest damage and recovery from catastrophic wind. Bot. Rev.
598     62, 113–185. https://doi.org/10.1007/BF02857920

599 Feal-Pérez, A., Blanco-Chao, R., Ferro-Vázquez, C., Martínez-Cortizas, A., Costa-Casais, M., 2014. Late-
600     Holocene storm imprint in a coastal sedimentary sequence (Northwest Iberian coast). The
601     Holocene 24, 477–488. https://doi.org/10.1177/0959683613520257

602 Feuillet, T., Chauveau, É., Pourinet, L., 2012. Xynthia est-elle exceptionnelle ? Réflexions sur
603     l'évolution et les temps de retour des tempêtes, des marées de tempête, et des risques de
604     surcotes associés sur la façade atlantique française. Norois n° 222, 27–44.

605 Frappier, A.B., Sahagian, D., Carpenter, S.J., González, L.A., Frappier, B.R., 2007. Stalagmite stable
606     isotope record of recent tropical cyclone events. Geology 35, 111–114.
607     https://doi.org/10.1130/G23145A.1

608 Gardner, T.A., Côté, I.M., Gill, J.A., Grant, A., Watkinson, A.R., 2005. Hurricanes and Caribbean Coral
609     Reefs: Impacts, Recovery Patterns, and Role in Long-Term Decline. Ecology 86, 174–184.
610     https://doi.org/10.1890/04-0141
611 Garnier, E., Ciavola, P., Spencer, T., Ferreira, O., Armaroli, C., McIvor, A., 2017. Historical analysis of
612     storm events: Case studies in France, England, Portugal and Italy. Coast. Eng.
613     https://doi.org/10.1016/j.coastaleng.2017.06.014
614 Gärtner, H., 2007. Tree roots — Methodological review and new development in dating and
615     quantifying erosive processes. Geomorphology 86, 243–251.
616     https://doi.org/10.1016/j.geomorph.2006.09.001
617 Gärtner, H., Schweingruber, F.H., Dikau, R., 2001. Determination of erosion rates by analyzing
618     structural changes in the growth pattern of exposed roots. Dendrochronologia 19, 81–91.
619 Goslin, J., Clemmensen, L.B., 2017. Proxy records of Holocene storm events in coastal barrier
620     systems: Storm-wave induced markers. Quat. Sci. Rev. 174, 80–119.
621     https://doi.org/10.1016/j.quascirev.2017.08.026
622 Gottschalk, M.K.E., 1977. Stormvloeden en rivieroverstromingen in Nederland, vol.3. Van Gorcum &
623     Comp, Assen/Amsterdam.
624 Grissino-Mayer, H.D., 2003. A Manual and Tutorial for the Proper Use of an Increment Borer. Tree-
625     Ring Res.
626 Hall, A.M., Hansom, J.D., Williams, D.M., Jarvis, J., 2006. Distribution, geomorphology and lithofacies
627     of cliff-top storm deposits: Examples from the high-energy coasts of Scotland and Ireland.
628     Mar. Geol. 232, 131–155. https://doi.org/10.1016/j.margeo.2006.06.008
629 Hansom, J.D., Hall, A.M., 2009. Magnitude and frequency of extra-tropical North Atlantic cyclones: A
630     chronology from cliff-top storm deposits. Quat. Int., Hurricanes and Typhoons: From the
631     Field Records to the Forecast 195, 42–52. https://doi.org/10.1016/j.quaint.2007.11.010
632 Hickey, K.R., 1997. Documentary records of coastal storms in Scotland, 1500- 1991 A.D. PhD Thesis
633     602.
634 Hippensteel, S.P., Martin, R.E., 1999. Foraminifera as an indicator of overwash deposits, Barrier
635     Island sediment supply, and Barrier Island evolution: Folly Island, South Carolina.
636     Palaeogeogr. Palaeoclimatol. Palaeoecol. 149, 115–125. https://doi.org/10.1016/S0031-
637     0182(98)00196-5
638 Hitz, O.M., Gärtner, H., Heinrich, I., Monbaron, M., 2008. Application of ash (Fraxinus excelsior L.)
639     roots to determine erosion rates in mountain torrents. CATENA 72, 248–258.
640     https://doi.org/10.1016/j.catena.2007.05.008
641 Hohl, R., Schweingruber, F.H., Schiesser, H.-H., 2002. Reconstruction of Severe Hailstorm Occurrence
642     with Tree Rings: A Case Study in Central Switzerland. Tree-Ring Res.
643 Hongo, C., 2018. The Hydrodynamic Impacts of Tropical Cyclones on Coral Reefs of Japan: Key Points
644     and Future Perspectives, in: Coral Reef Studies of Japan, Coral Reefs of the World. Springer,
645     Singapore, pp. 163–173.
646 Kenney, W.F., Brenner, M., Arnold, T.E., Curtis, J.H., Schelske, C.L., 2016. Sediment cores from
647     shallow lakes preserve reliable, informative paleoenvironmental archives despite hurricane-
648     force winds. Ecol. Indic. 60, 963–969. https://doi.org/10.1016/j.ecolind.2015.08.046
649 Lafon, C.W., Speer, J.H., 2002. Using dendrochronology to identify major ice storm events in oak
650     forests of southwestern Virginia. Clim. Res. 20, 41–54.
651 Lamb, H., Frydendahl, K., 1991. Historic Storms of the North Sea, British Isles and Northwest Europe.
652     Cambridge University Press.
653 Lamb, H.H., 1995. Climate, History and the Modern World, 2 edition. ed. Routledge, London.
654 Le Roy, S., Pedreros, R., André, C., Paris, F., Lecacheux, S., Marche, F., Vinchon, C., 2015. Coastal
655     flooding of urban areas by overtopping: dynamic modelling application to the Johanna storm
656     (2008) in Gâvres (France). Nat Hazards Earth Syst Sci 15, 2497–2510.
657     https://doi.org/10.5194/nhess-15-2497-2015
658 Lima, A.L., Hubeny, J.B., Reddy, C.M., King, J.W., Hughen, K.A., Eglinton, T.I., 2005. High-resolution
659     historical records from Pettaquamscutt River basin sediments: 1. 210Pb and varve

19

660             chronologies validate record of 137Cs released by the Chernobyl accident. Geochim.
661             Cosmochim. Acta 69, 1803–1812. https://doi.org/10.1016/j.gca.2004.10.009

662 Liu, K., 2004. Paleotempestology: Geographic Solutions to Hurricane Hazard Assessment and Risk
663             Prediction, in: Janelle, D.G., Warf, B., Hansen, K. (Eds.), WorldMinds: Geographical
664             Perspectives on 100 Problems. Springer, Dordrecht, pp. 443–448.

665 Liu, K., Fearn, M.L., 2000. Reconstruction of Prehistoric Landfall Frequencies of Catastrophic
666             Hurricanes in Northwestern Florida from Lake Sediment Records. Quat. Res. 54, 238–245.
667             https://doi.org/10.1006/qres.2000.2166

668 Liu, K., Fearn, M.L., 1993. Lake-sediment record of late Holocene hurricane activities from coastal
669             Alabama. Geology 21, 793–796. https://doi.org/10.1130/0091-
670             7613(1993)021<0793:LSROLH>2.3.CO;2

671 Lomenick, T.F., Tamura, T., 1965. Naturally Occurring Fixation of Cesium-137 on Sediments of
672             Lacustrine Origin. Soil Sci. Soc. Am. J. 29, 383–387.
673             https://doi.org/10.2136/sssaj1965.03615995002900040012x

674 Lozano, I., Devoy, R.J.N., May, W., Andersen, U., 2004. Storminess and vulnerability along the Atlantic
675             coastlines of Europe: analysis of storm records and of a greenhouse gases induced climate
676             scenario. Mar. Geol., Storms and their significance in coastal morpho-sedimentary dynamics
677             210, 205–225. https://doi.org/10.1016/j.margeo.2004.05.026

678 Lu, H., An, Z., 1998. Paleoclimatic significance of grain size of loess-palaeosol deposit in Chinese Loess
679             Plateau. Sci. China Ser. Earth Sci. 41, 626–631. https://doi.org/10.1007/BF02878745

680 Malik, I., 2008. Dating of small gully formation and establishing erosion rates in old gullies under
681             forest by means of anatomical changes in exposed tree roots (Southern Poland).
682             Geomorphology 93, 421–436. https://doi.org/10.1016/j.geomorph.2007.03.007

683 Martin, J.-P., Germain, D., 2016. Can we discriminate snow avalanches from other disturbances using
684             the spatial patterns of tree-ring response? Case studies from the Presidential Range, White
685             Mountains, New Hampshire, United States. Dendrochronologia 37, 17–32.
686             https://doi.org/10.1016/j.dendro.2015.12.004

687 Martin, L., Mooney, S., Goff, J., 2014. Coastal wetlands reveal a non-synchronous island response to
688             sea-level change and a palaeostorm record from 5.5 kyr to present. The Holocene 24, 569–
689             580. https://doi.org/10.1177/0959683614522306

690 May, S.M., Brill, D., Leopold, M., Callow, J.N., Engel, M., Scheffers, A., Opitz, S., Norpoth, M.,
691             Brückner, H., 2017. Chronostratigraphy and geomorphology of washover fans in the Exmouth
692             Gulf (NW Australia) – A record of tropical cyclone activity during the late Holocene. Quat. Sci.
693             Rev. 169, 65–84. https://doi.org/10.1016/j.quascirev.2017.05.023

694 Migeon, S., Weber, O., Faugeres, J.-C., Saint-Paul, J., 1998. SCOPIX: A new X-ray imaging system for
695             core analysis. Geo-Mar. Lett. 18, 251–255. https://doi.org/10.1007/s003670050076

696 Mix, A.C., Harris, S.E., Janecek, T.R., 1995. Estimating lithology from nonintrusive reflectance spectra :
697             Leg 138.

698 Naquin, J.D., Liu, K., McCloskey, T.A., Bianchette, T.A., 2014. Storm deposition induced by hurricanes
699             in a rapidly subsiding coastal zone. J. Coast. Res. 308–313. https://doi.org/10.2112/SI70-
700             052.1

701 Nodine, E.R., Gaiser, E.E., 2015. Seasonal differences and response to a tropical storm reflected in
702             diatom assemblage changes in a southwest Florida watershed. Ecol. Indic. 57, 139–148.
703             https://doi.org/10.1016/j.ecolind.2015.04.035

704 Noren, A.J., Bierman, P.R., Steig, E.J., Lini, A., Southon, J., 2002. Millennial-scale storminess variability
705             in the northeastern United States during the Holocene epoch. Nature 419, 821–824.
706             https://doi.org/10.1038/nature01132

707 Olthof, I., King, D.J., Lautenschlager, R.A., 2003. Overstory and understory leaf area index as
708             indicators of forest response to ice storm damage. Ecol. Indic. 3, 49–64.
709             https://doi.org/10.1016/S1470-160X(03)00010-4

710    Orme, L.C., Davies, S.J., Duller, G. a. T., 2015. Reconstructed centennial variability of Late Holocene
711        storminess from Cors Fochno, Wales, UK. J. Quat. Sci. 30, 478–488.
712        https://doi.org/10.1002/jqs.2792
713    Parsons, M.L., 1998. Salt Marsh Sedimentary Record of the Landfall of Hurricane Andrew on the
714        Louisiana Coast: Diatoms and Other Paleoindicators. J. Coast. Res. 14, 939–950.
715        https://doi.org/10.2307/4298846
716    Peng, Y., Xiao, J., Nakamura, T., Liu, B., Inouchi, Y., 2005. Holocene East Asian monsoonal
717        precipitation pattern revealed by grain-size distribution of core sediments of Daihai Lake in
718        Inner Mongolia of north-central China. Earth Planet. Sci. Lett. 233, 467–479.
719        https://doi.org/10.1016/j.epsl.2005.02.022
720    Pierce, J.W., 1970. Tidal Inlets and Washover Fans. J. Geol. 78, 230–234.
721        https://doi.org/10.1086/627504
722    Polonia, A., Bonatti, E., Camerlenghi, A., Lucchi, R.G., Panieri, G., Gasperini, L., 2013. Mediterranean
723        megaturbidite triggered by the AD 365 Crete earthquake and tsunami. Sci. Rep. 3, 1285.
724        https://doi.org/10.1038/srep01285
725    Pouzet, P., Creach, A., Godet, L., 2015. Dynamique de la démographie et du bâti dans l'ouest du
726        Marais poitevin depuis 1705. Norois Environ. Aménage. Société 83–96.
727        https://doi.org/10.4000/norois.5589
728    Pouzet, P., Maanan, M., Schmidt, S., Athimon, E., Robin, M., 2018. Three centuries of historical and
729        geological data for the marine deposit reconstruction: examples from French Atlantic coast.
730        Mar. Geol. Submitted.
731    Ritchie, J.C., McHenry, J.R., 1990. Application of Radioactive Fallout Cesium-137 for Measuring Soil
732        Erosion and Sediment Accumulation Rates and Patterns: A Review. J. Environ. Qual. 19, 215–
733        233. https://doi.org/10.2134/jeq1990.00472425001900020006x
734    Rovera, G., Lopez Saez, J., Corona, C., Stoffel, M., Berger, F., 2013. Preliminary quantification of the
735        erosion of sandy-gravelly cliffs on the island of Porquerolles (Provence, France) through
736        dendrogeomorphology, using exposed roots of Aleppo pine (Pinus halepensis Mill.). Geogr.
737        Fis. E Din. Quat. 36, 181–187.
738    Roy, P.D., Caballero, M., Lozano, R., Ortega, B., Lozano, S., Pi, T., Israde, I., Morton, O., 2010.
739        Geochemical record of Late Quaternary paleoclimate from lacustrine sediments of paleo-lake
740        San Felipe, western Sonora Desert, Mexico. J. South Am. Earth Sci. 29, 586–596.
741        https://doi.org/10.1016/j.jsames.2009.11.009
742    Sabatier, P., Dezileau, L., Briqueu, L., Colin, C., Siani, G., 2010. Paleostorm events revealed by clay
743        minerals and geochemistry in coastal lagoon: a study case of Pierre Blanche (NW
744        Mediterranean Sea). Sediment. Geol. 228, 205–217.
745    Sabatier, P., Dezileau, L., Colin, C., Briqueu, L., Bouchette, F., Martinez, P., Siani, G., Raynal, O., Von
746        Grafenstein, U., 2012. 7000 years of paleostorm activity in the NW Mediterranean Sea in
747        response to Holocene climate events. Quat. Res. 77, 1–11.
748        https://doi.org/10.1016/j.yqres.2011.09.002
749    Sabatier, P., Dezileau, L., Condomines, M., Briqueu, L., Colin, C., Bouchette, F., Le Duff, M.,
750        Blanchemanche, P., 2008. Reconstruction of paleostorm events in a coastal lagoon (Hérault,
751        South of France). Mar. Geol. 251, 224–232. https://doi.org/10.1016/j.margeo.2008.03.001
752    Schweingruber, F.H., 1996. Tree rings and environment dendroecology. Haupt,
753        Berne ;Stuttgart ;Vienna.
754    Scoffin, T.P., 1993. The geological effects of hurricanes on coral reefs and the interpretation of storm
755        deposits. Coral Reefs 12, 203–221. https://doi.org/10.1007/BF00334480
756    Scott, D.B., Collins, E.S., Gayes, P.T., Wright, E., 2003. Records of prehistoric hurricanes on the South
757        Carolina coast based on micropaleontological and sedimentological evidence, with
758        comparison to other Atlantic Coast records. GSA Bull. 115, 1027–1039.
759        https://doi.org/10.1130/B25011.1
760    Shroder, J., 1980. Dendrogeomorphology: review and new techniques of tree-ring dating. Prog. Phys.
761        Geogr. Earth Environ. 4, 161–188. https://doi.org/10.1177/030913338000400202

762 Shroder, J.F., 1978. Dendrogeomorphological Analysis of Mass Movement on Table Cliffs Plateau,
763     Utah. Quat. Res. 9, 168–185. https://doi.org/10.1016/0033-5894(78)90065-0

764 Speer, J.H., 2012. Fundamentals of Tree Ring Research, 2 edition. ed. University of Arizona Press,
765     Tucson, Ariz.

766 Stager, J.C., Cumming, B.F., Laird, K.R., Garrigan-Piela, A., Pederson, N., Wiltse, B., Lane, C.S., Nester,
767     J., Ruzmaikin, A., 2017. A 1600-year diatom record of hydroclimate variability from Wolf
768     Lake, New York. The Holocene 27, 246–257. https://doi.org/10.1177/0959683616658527

769 Steers, J.A., Stoddart, D.R., Bayliss-Smith, T.P., Spencer, T., Durbidge, P.M., 1979. The Storm Surge of
770     11 January 1978 on the East Coast of England. Geogr. J. 145, 192–205.
771     https://doi.org/10.2307/634386

772 Switzer, A.D., Jones, B.G., 2008. Large-scale washover sedimentation in a freshwater lagoon from the
773     southeast Australian coast: sea-level change, tsunami or exceptionally large storm? The
774     Holocene 18, 787–803. https://doi.org/10.1177/0959683608089214

775 Travis, D., Meentemeyer, V., 1991. Influence of glaze ice storms on growth rates of loblolly pine Pinus
776     taeda and shortleaf pine Pinus echinata in the Southern Appalachian Piedmont. Clim. Res. -
777     Clim. RES 1, 199–205. https://doi.org/10.3354/cr001199

778 Walling, D.E., He, Q., 1999. Improved Models for Estimating Soil Erosion Rates from Cesium-137
779     Measurements. J. Environ. Qual. 28, 611–622.
780     https://doi.org/10.2134/jeq1999.00472425002800020027x

781 Wang, P., Horwitz, M.H., 2007. Erosional and depositional characteristics of regional overwash
782     deposits caused by multiple hurricanes. Sedimentology 54, 545–564.
783     https://doi.org/10.1111/j.1365-3091.2006.00848.x

784 Wassmer, P., Schneider, J.-L., Fonfrège, A.-V., Lavigne, F., Paris, R., Gomez, C., 2010. Use of
785     anisotropy of magnetic susceptibility (AMS) in the study of tsunami deposits: Application to
786     the 2004 deposits on the eastern coast of Banda Aceh, North Sumatra, Indonesia. Mar. Geol.
787     275, 255–272. https://doi.org/10.1016/j.margeo.2010.06.007

788 Yu, K.-F., Zhao, J.-X., Shi, Q., Meng, Q.-S., 2009. Reconstruction of storm/tsunami records over the
789     last 4000 years using transported coral blocks and lagoon sediments in the southern South
790     China Sea. Quat. Int. 195, 128–137. https://doi.org/10.1016/j.quaint.2008.05.004

791 Zecchetto, S., Umgiesser, G., Brocchini, M., 1997. Hindcast of a storm surge induced by local real
792     wind fields in the Venice Lagoon. Cont. Shelf Res. 17, 1513–1538.
793     https://doi.org/10.1016/S0278-4343(97)00023-X

794 Zhu, Z., Feinberg, J.M., Xie, S., Bourne, M.D., Huang, C., Hu, C., Cheng, H., 2017. Holocene ENSO-
795     related cyclic storms recorded by magnetic minerals in speleothems of central China. Proc.
796     Natl. Acad. Sci. 114, 852–857. https://doi.org/10.1073/pnas.1610930114
797

798 Primary Sources of historical archives:

799    -   Meteo France :

800 http://tempetes.meteo.fr/Tempete-du-12-mars-1967.html

801 http://tempetes.meteofrance.fr/Tempete-du-13-fevrier-1972.html

802 http://tempetes.meteo.fr/Tempete-du-15-decembre-1979.html

803 http://tempetes.meteofrance.fr/Daria-le-25-janvier-1990.html

804    http://tempetes.meteofrance.fr/Herta-le-03-fevrier-1990.html

805    http://tempetes.meteofrance.fr/Viviane-du-26-au-28-fevrier-1990.html

806    -    Nantes Municipal Archives  Nantes :

807    1038 W 327

808    23 Z 355

809    24 PRES 152, 05/02/1990, Presse Océan

810    24 PRES 152, 27-28/02/1990, Presse Océan

811    -    Departmental archives of Vendée :

812    1856 W 38

813    78/31 1953-1975 – tempête du 13 février 1972

814    -    Other :

815    Le Marin 20 Janvier 1978 N°1595

816    MetMar 1978 N°101

817 Fig. 1. Study area. A. General overview; B. Forested area on Pen Bron dune; C. Traict du
818 Croizic back barrier

819 Fig. 2. Wind activity at the study site from reanalysis data

820 Fig. 3. Tree-ring patterns in A. Trees not affected by strong episodic winds; B. Trees affected
821 by strong winds during episodic storms; C. Schematic representation of growth rings of the C
822 and D axes of one tree over time and their signals due to strong winds during storms

823 Fig. 4. Sedimentological results

824 Fig. 5. Temporal distribution of tree-ring disturbances (reaction wood occurrence and storm
825 signals) and calculation details of the Index of Storm Disturbance

826 Fig. 6. Index of Storm Disturbance over time

827 Fig. 7. The ten highest wind speed records from November 1993 to October 2012, calculated
828 from reanalysis data

829 Fig. 8. Characterization of annual winds from November 1993 to October 2012, calculated
830 from reanalysis data, and percentage of SW winds

831 Fig. 9. Intense (A) and extreme (B) wind records per tree years from November 1993 to
832 October 2012, calculated from reanalysis data

833 Fig. 10. Winds recorded during the storms of March 13, 1967 (A), February 13, 1972 (B) and
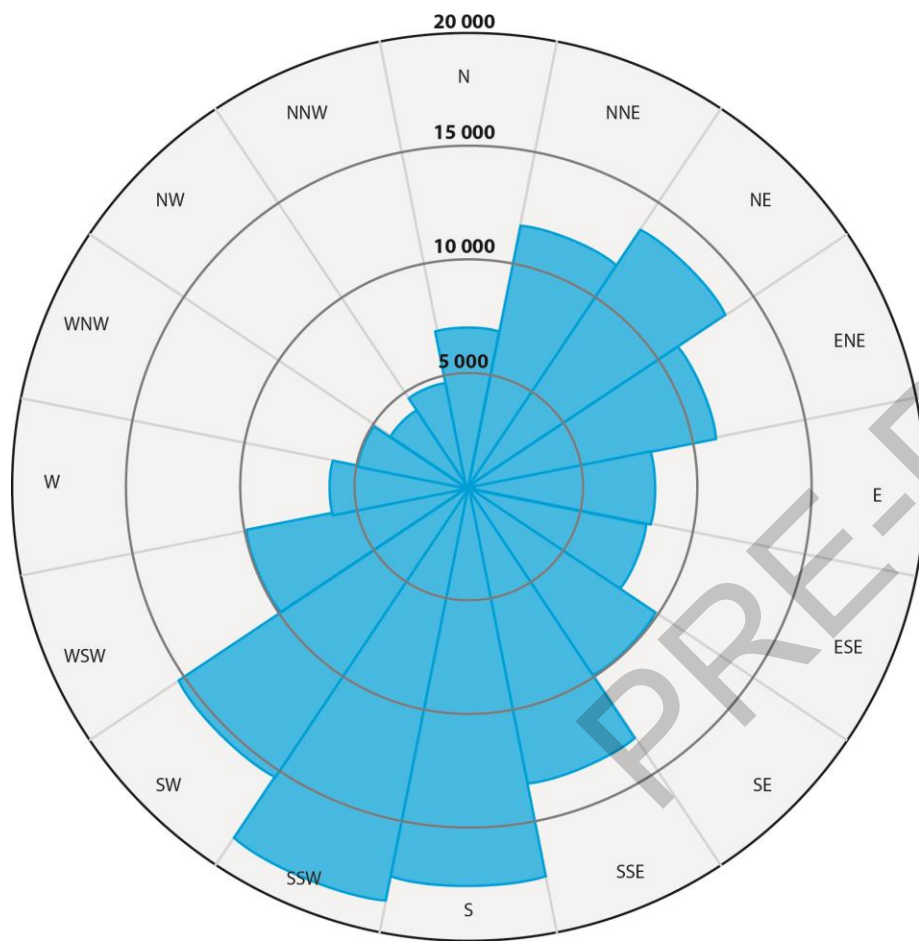834 December 15, 1979 (C), from Meteo France

835

836

Fig. 1

## A. Number of prevailing winds
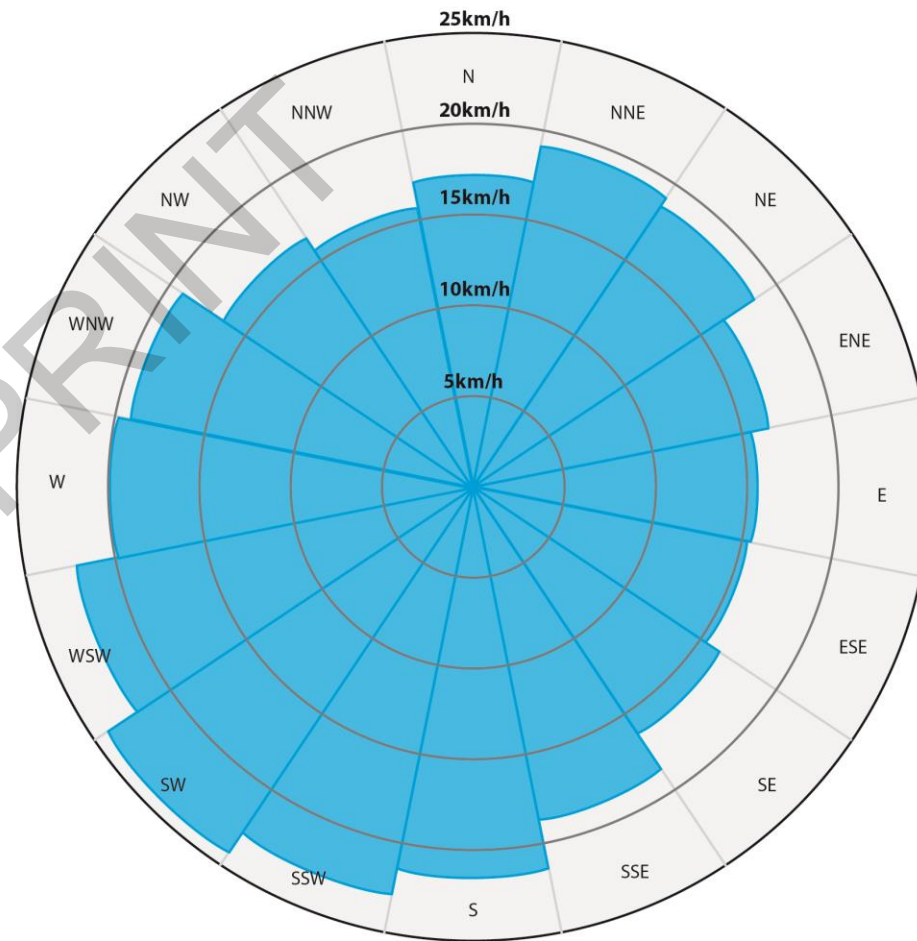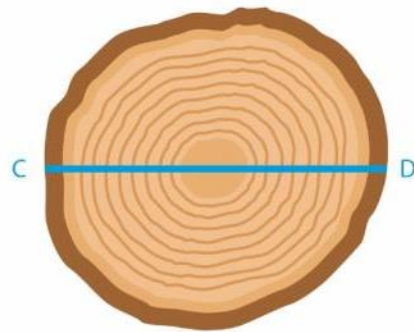


## B. Average speeds of prevailing winds
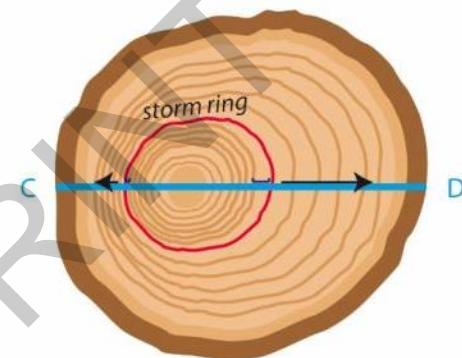
Fig. 2

1

Fig. 3

## Tree evolution

## Tree-ring patterns

### A. Stand undisturbed by winds



### B. Stand disturbed by strong winds



— Observable disproportions for the same tree year   ➔ Eccentricity growth   ▬ Sample axes

(Created with Freepik © templates)

### C. Example of storm-type signal identified in tree-ring widths
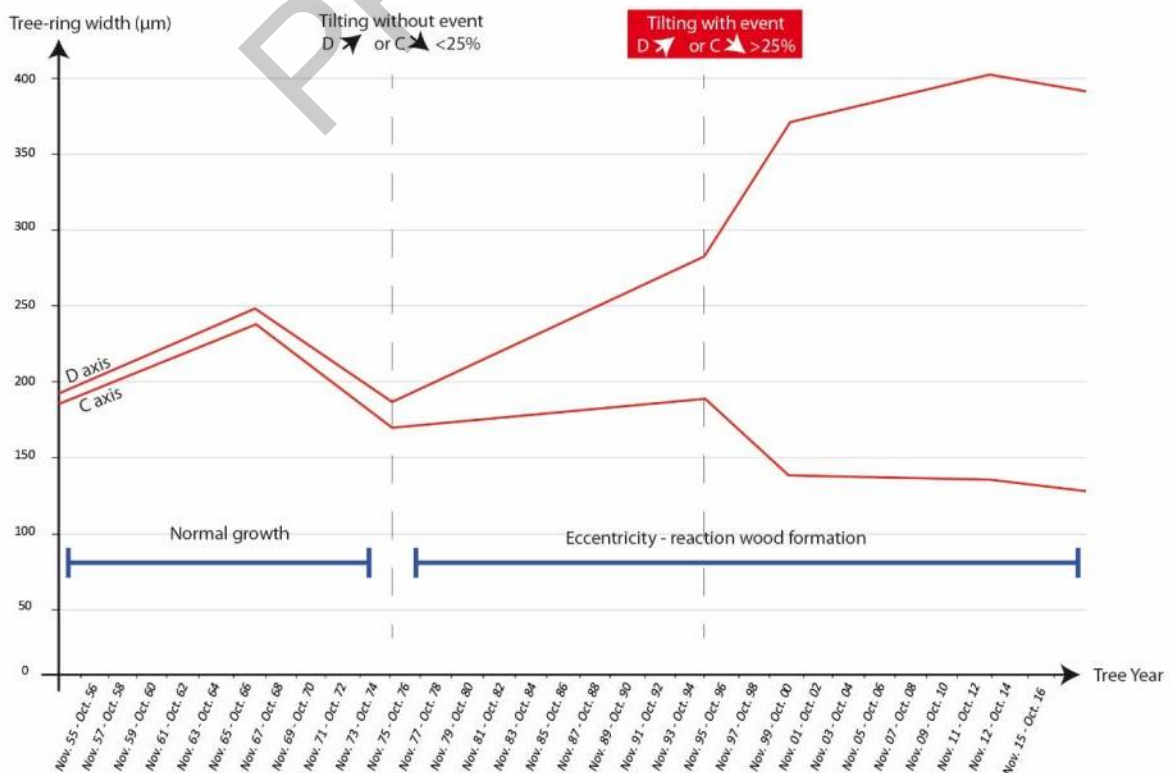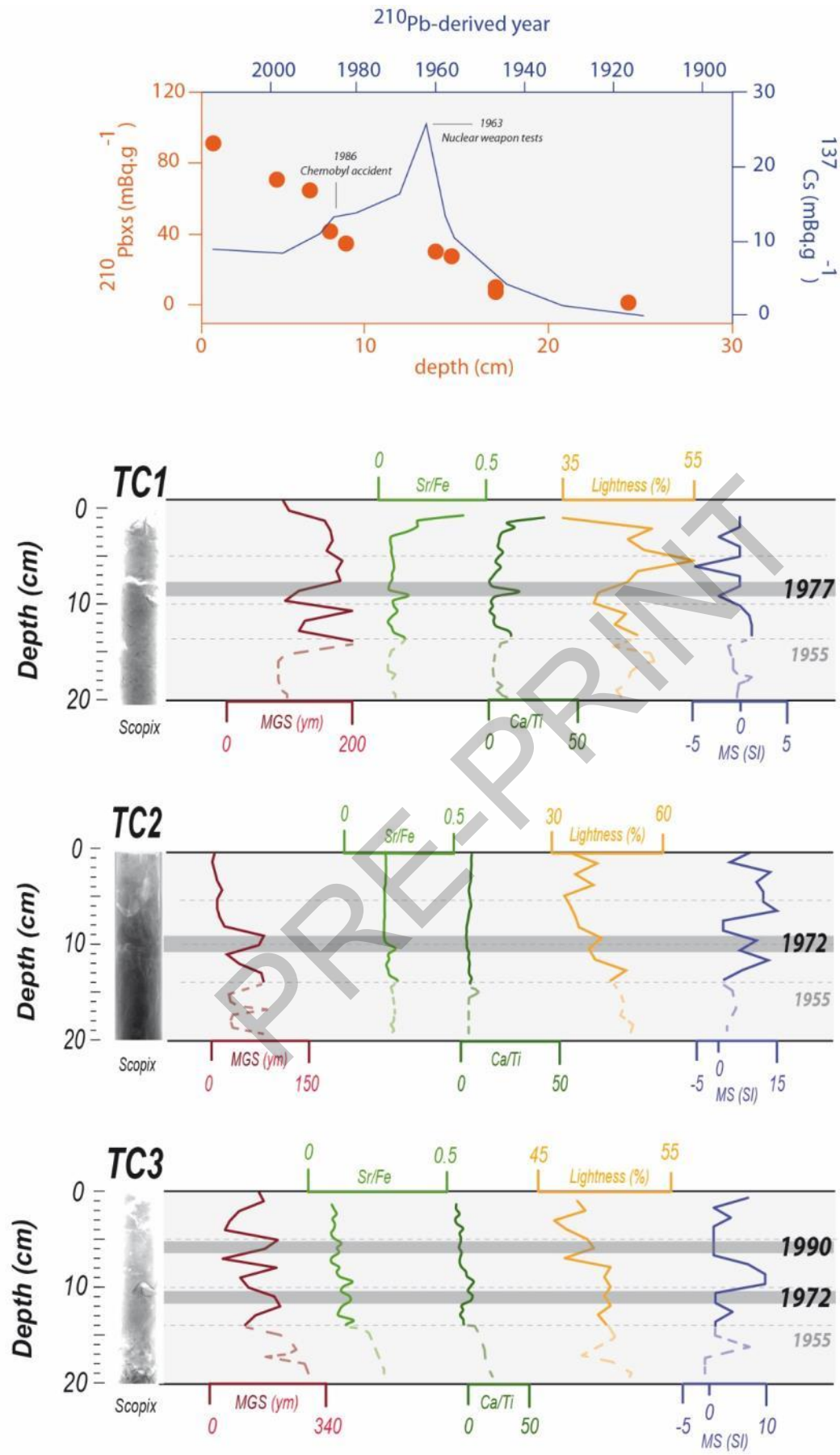
Fig. 4



1940 : Dates AD found with dating in sedimentological and historical archives for probable extreme wave event
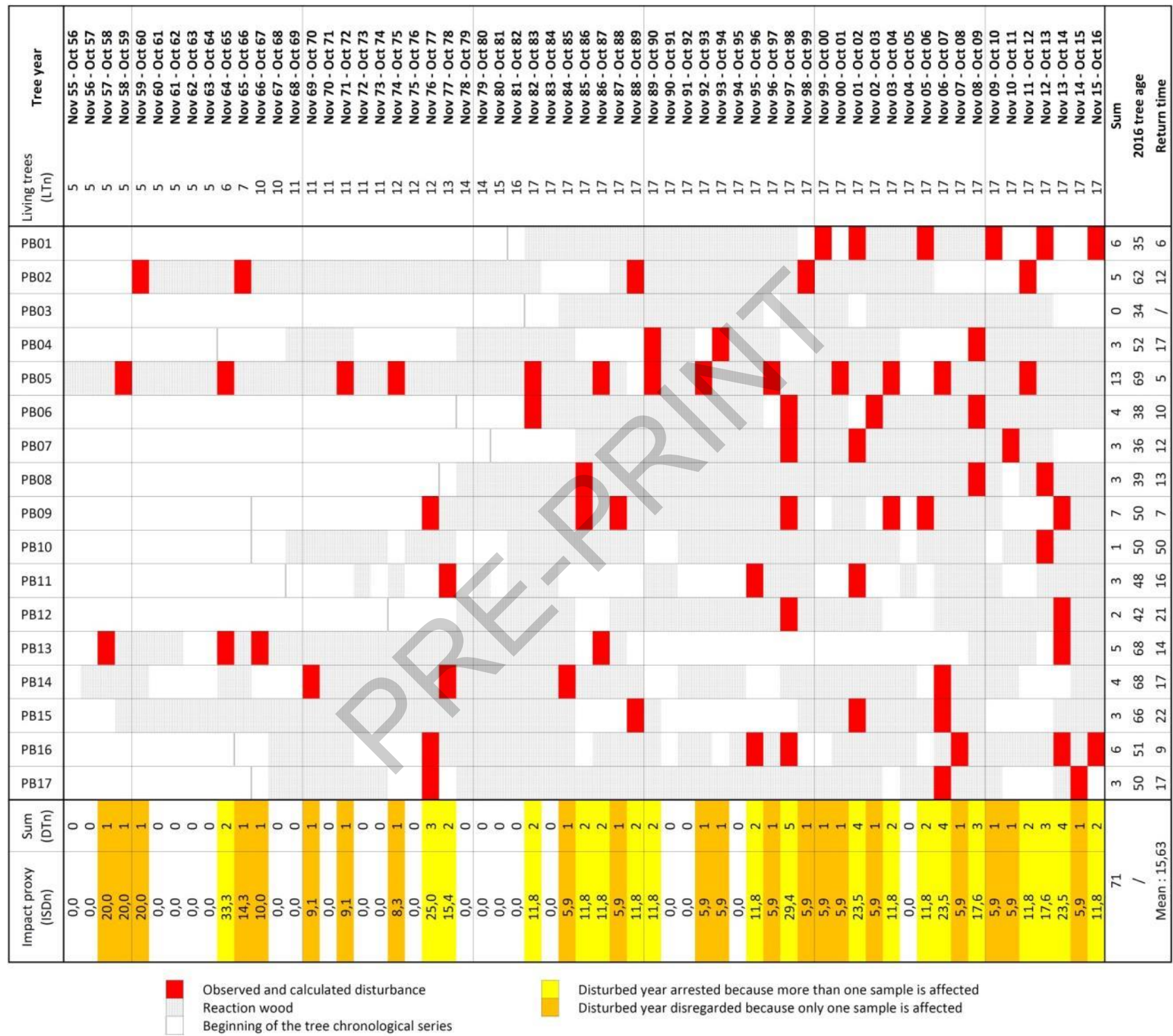
Fig. 5

Observed and calculated disturbance

Reaction wood

Beginning of the tree chronological series

Disturbed year arrested because more than one sample is affected

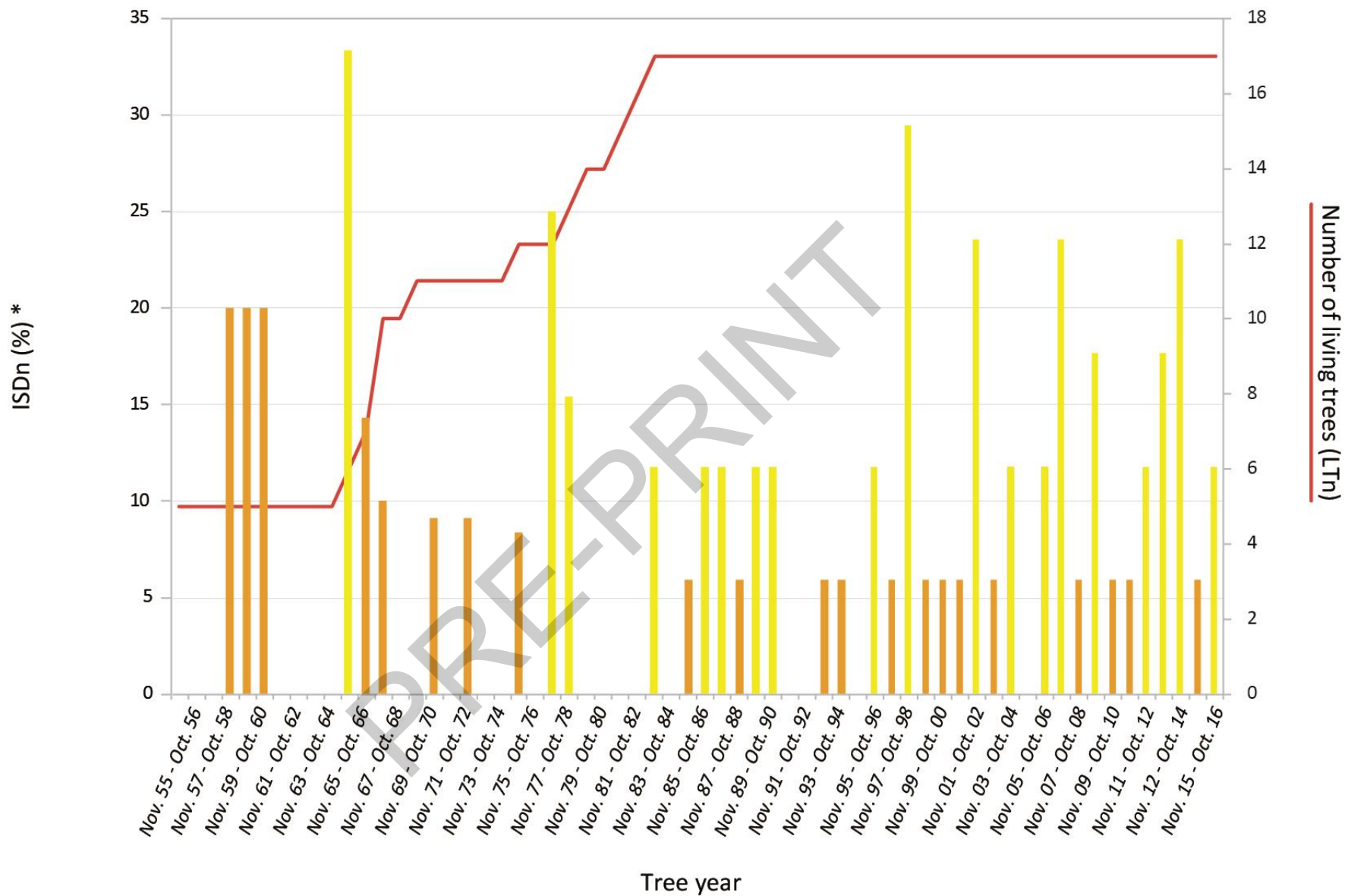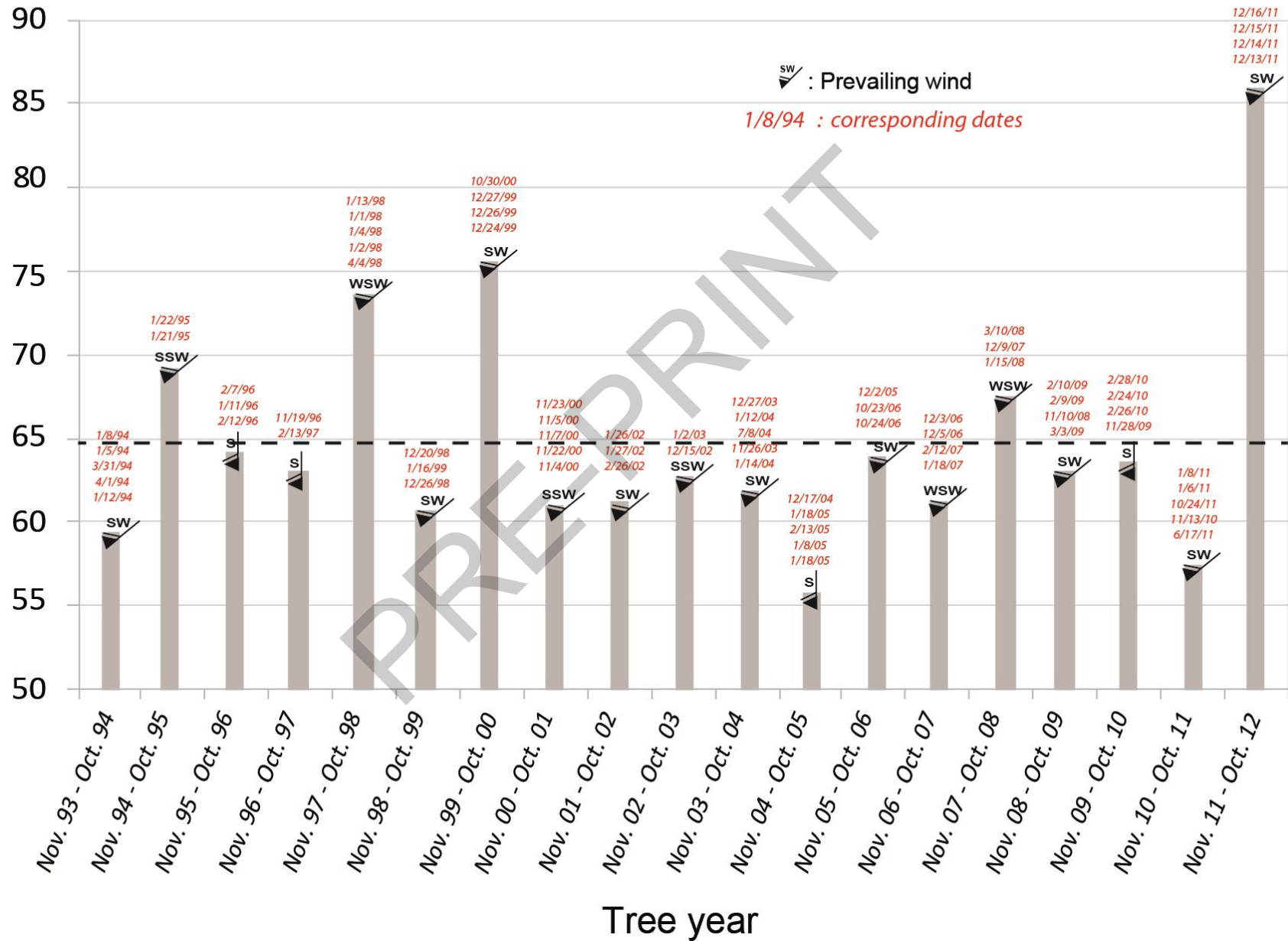Disturbed year disregarded because only one sample is affected

Fig. 6



*Disturbed year arrested because of more than one sample is affected

*Disturbed year disregarded because only one sample is affected

Fig. 7

# Average for the ten highest winds of each tree year (km/h)
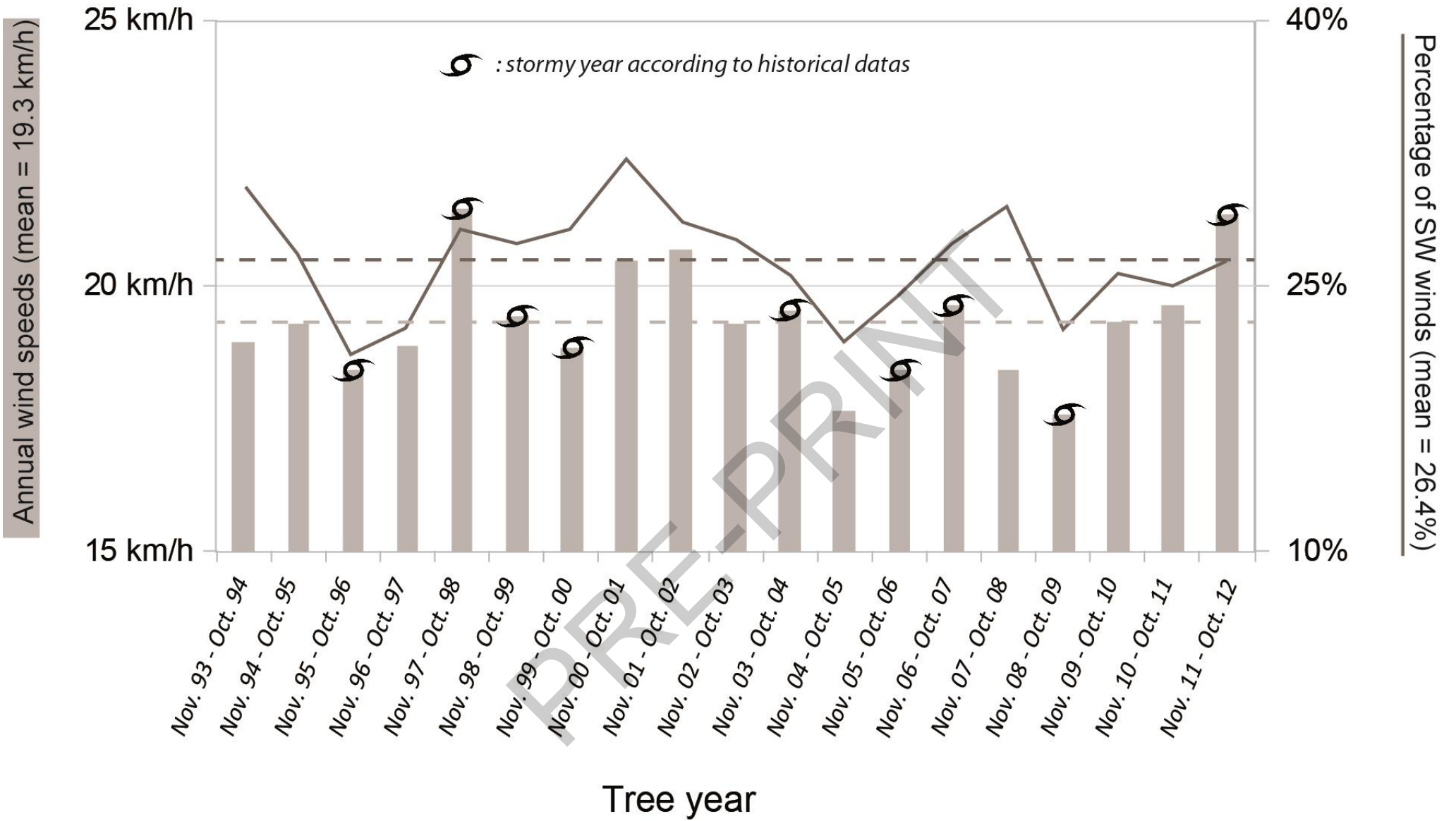## (mean = 64.9 km/h)

Fig. 8

A. Intense wind speeds :

*Number superiors to the 9th decile*
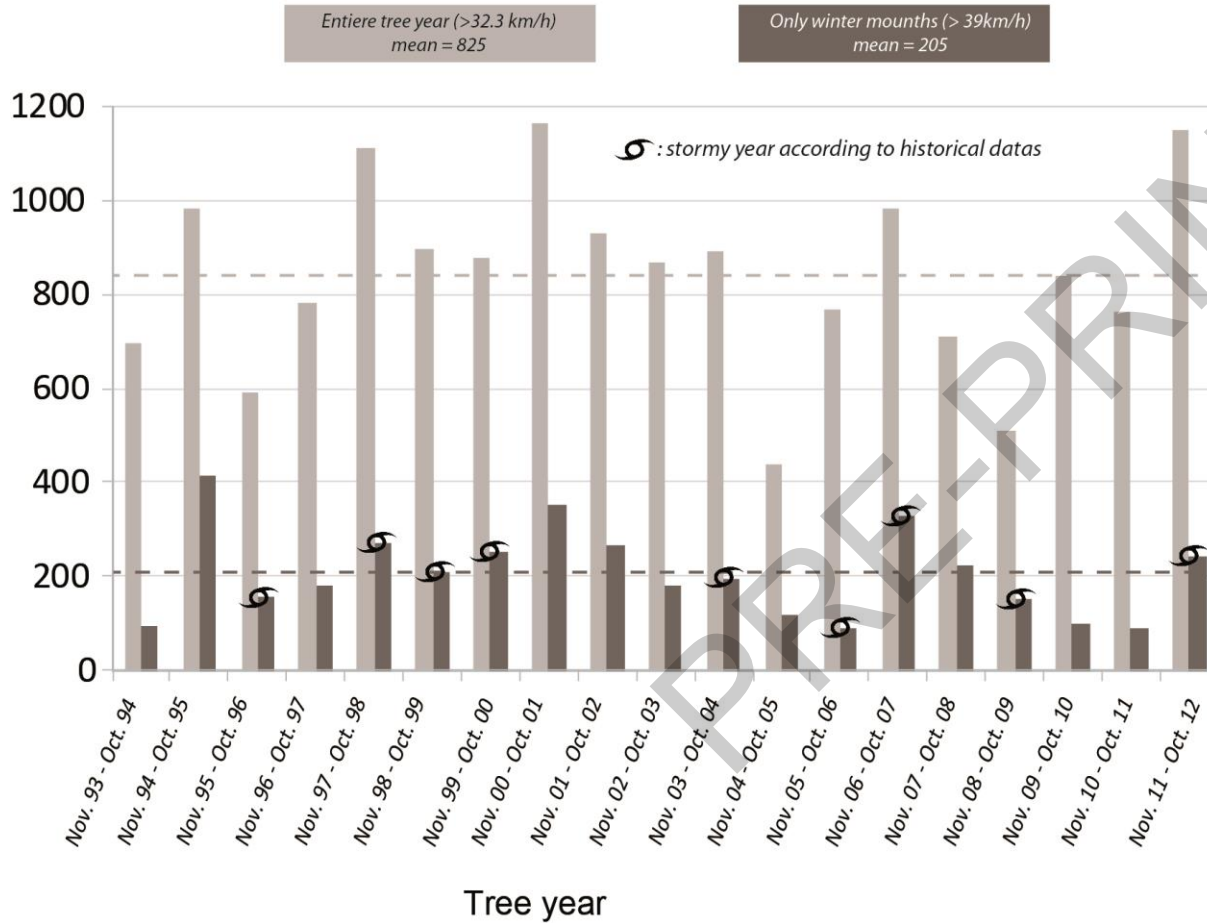
B. Extreme wind speeds :

*Number superior to the Beaufort 9 rank (75 km/h)*

Fig. 9

Fig. 10



A. Two-day maximum instant wind speeds
3/13/67
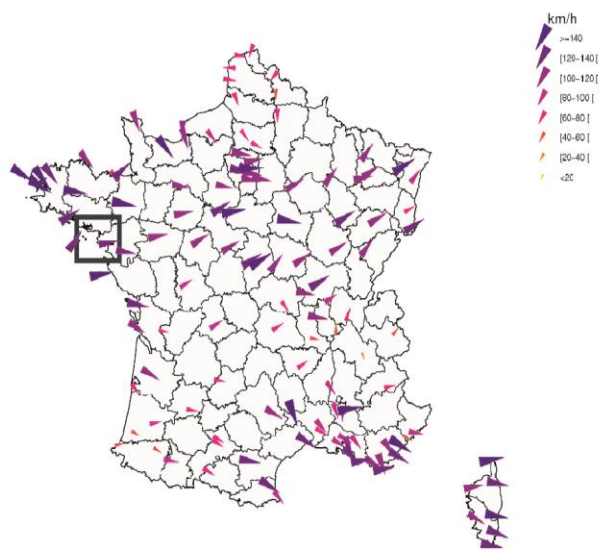
B. Daily maximum instant wind speeds
2/13/72
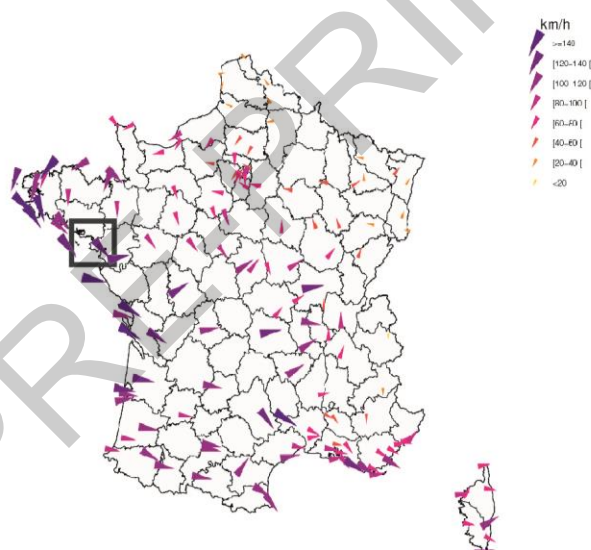
C. Daily maximum instant wind speeds
12/15/79

☐ Study site

Table 1. Coordinates of each sedimentological and dendrochronological core

Table 2. Comparison of Tree Ring Width results per tree years with recent storm inventoried in historical data

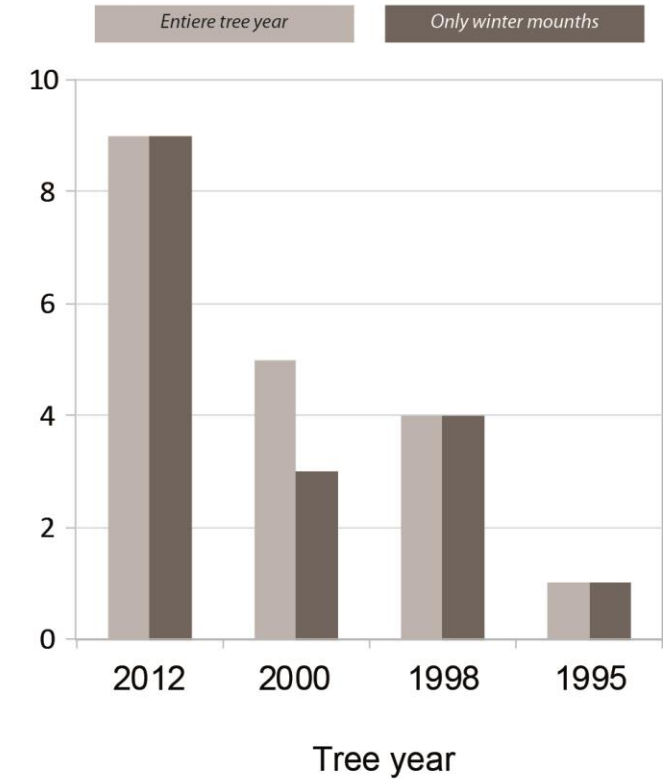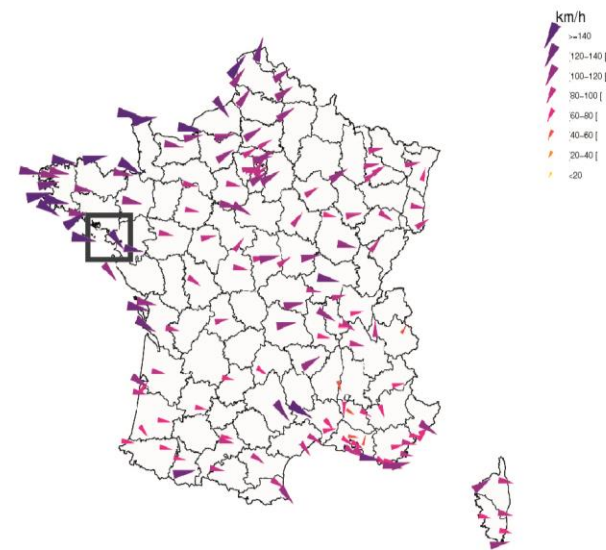| Sedimentological cores | | | | |
|---|---|---|---|---|
| Name | Id | X (RGF lambert 93) | Y (RGF lambert 93) | Maximum Depth (cm) |
| Traict du Croisic 1 | TC1 | 285140.145 | 6704373.272 | 84 |
| Traict du Croisic 2 | TC2 | 284667.764 | 6704419.583 | 71 |
| Traict du Croisic 3 | TC3 | 284877.807 | 6704445.014 | 85 |
| Dendrochronological cores | | | | |
| Name | Id | X (RGF lambert 93) | Y (RGF lambert 93) | Disturbance direction |
| Pen Bron 1 | PB01 | 284990.395 | 6705920.372 | SW>NE |
| Pen Bron 2 | PB02 | 284915.957 | 6705848.237 | SW>NE |
| Pen Bron 3 | PB03 | 284953.042 | 6705867.302 | N.NW>S.SE |
| Pen Bron 4 | PB04 | 284977.943 | 6705862.471 | S.SW>N.NE |
| Pen Bron 5 | PB05 | 284945.743 | 6705883.276 | S.SW>N.NE |
| Pen Bron 6 | PB06 | 284867.653 | 6705758.813 | S.SW>N.NE |
| Pen Bron 7 | PB07 | 284915.957 | 6705822.005 | SW>NE |
| Pen Bron 8 | PB08 | 284945.743 | 6705883.276 | S.SW>N.NE |
| Pen Bron 9 | PB09 | 284938.66 | 6705902.329 | W>E |
| Pen Bron 10 | PB10 | 284955.673 | 6705935.167 | S>N |
| Pen Bron 11 | PB11 | 284960.503 | 6705944.109 | S>N |
| Pen Bron 12 | PB12 | 284969.626 | 6705893.983 | S.SW>N.NE |
| Pen Bron 13 | PB13 | 284985.135 | 6705905.273 | SW>NE |
| Pen Bron 14 | PB14 | 284990.395 | 6705893.983 | SW>NE |
| Pen Bron 15 | PB15 | 284983.257 | 6705908.498 | W.NW>E.SE |
| Pen Bron 16 | PB16 | 284973.382 | 6705887.535 | SW>NE |
| Pen Bron 17 | PB17 | 284973.382 | 6705886.513 | SW>NE |

Table 1

| Tree year (from Nov. N-1 to Oct. N) | ISD | Known storm* | Compatibility | Storm dates (month/day/year) | Main Historical Sources |
|---|---|---|---|---|---|
| 2016 | 11,8 | Yes | Yes | 2/8/16 | http://www.ouest-france.fr/meteo/tempete/meteo-tempete-sur-louest-139-km/h-de-vent-en-bretagne-et-normandie-4024680 |
| 2015 | 5,9 | No | Yes | / | / |
| 2014 | 23,5 | Several | Yes | 2/14/14<br>2/1/14<br>12/23/13 | Archives Départementales de Loire-Atlantique, PR 967 849, du 15-16/02/2014<br>Archives Départementales de Loire-Atlantique, PR 967 849, du 04/02/2014<br>http://tempetes.meteo.fr/Tempete-Dirk-de-noel-2013.html |
| 2013 | 17,6 | Yes | Yes | 10/27/13 | http://www.lemonde.fr/planete/article/2013/10/27/tempete-12-departements-du-nord-ouest-en-alerte-orange_3503693_3244.html |
| 2012 | 11,8 | Yes | Yes | 12/6/11 | http://tempetes.meteo.fr/Tempete-Joachim-du-16-decembre-2011.html |
| 2011 | 5,9 | No | Yes | / | |
| 2010 | 5,9 | Probably | ? | 2/27/10 | http://tempetes.meteo.fr/Tempete-Xynthia-du-27-au-28-fevrier-2010.html |
| 2009 | 17,6 | Yes | Yes | 2/9/09 | http://tempetes.meteo.fr/Tempete-Quinten-du-09-au-10-fevrier-2009.html |
| 2008 | 5,9 | MI | Yes | 3/9/08 | Archives départementales de Vendée, BIB PE 20/652, Ouest France édition Vendée Ouest, 11/03/2008 p 1,6,7,9 |
| 2007 | 23,5 | Yes | Yes | 12/8/06 | http://tempetes.meteo.fr/Tempete-Vera-le-8-decembre-2006.html |
| 2006 | 11,8 | Yes | Yes | 12/1/05 | Archives Départementales de Loire-Atlantique, PR 967 650, du 04/12/2005 |
| 2005 | 0,0 | No | Yes | / | |
| 2004 | 11,8 | Yes | Yes | 1/12/04 | http://tempetes.meteo.fr/Tempetes-successives-du-12-au-15-janvier-2004.html |
| 2003 | 5,9 | Probably | ? | 1/2/03 | http://tempetes.meteo.fr/Tempete-Calvann-du-02-janvier-2003.html |
| 2002 | 23,5 | No | No | / | |
| 2001 | 5,9 | No | Yes | / | |
| 2000 | 5,9 | Several | No | 10/30/00<br>12/27/99<br>12/26/99 | http://tempetes.meteo.fr/Tempete-Oratia-du-30-octobre-2000.html<br>http://tempetes.meteo.fr/Martin-les-27-et-28-decembre-1999.html<br>http://tempetes.meteo.fr/Lothar-le-26-decembre-1999.html |
| 1999 | 5,9 | Yes | No | 12/20/98 | Archives Départementales de Loire-Atlantique PR 967 483 du 21/12/1998 |
| 1998 | 29,4 | Several | Yes | 1/13/98<br>1/4/98<br>1/2/98 | Archives municipales de Nantes,26PRESSE245, Ouest-France du 14/01/1998<br>http://tempetes.meteo.fr/Tempete-du-4-janvier-1998.html<br>http://tempetes.meteo.fr/Tempete-du-2-janvier-1998.html |
| 1997 | 5,9 | No | Yes | / | |
| 1996 | 11,8 | Yes | Yes | 2/7/96 | http://tempetes.meteo.fr/Tempete-du-7-et-8-fevrier-1996.html |
| 1995 | 0,0 | No | Yes | / | |
| 1994 | 5,9 | MI | Yes | 1/5/94 | http://tempetes.meteo.fr/Tempetes-du-5-au-7-janvier-1994.html |
| 1993 | 5,9 | MI | Yes | 9/12/93 | http://tempetes.meteo.fr/Tempete-des-12-et-13-septembre-1993.html |
| 1992 | 0,0 | Probably | ? | 12/18/91 | http://tempetes.meteo.fr/Synthese-du-18-au-25-decembre-1991.html |
| 1991 | 0,0 | No | Yes | / | |
| 1990 | 11,8 | Several | Yes | 2/26/1990<br>2/3/1990<br>1/25/1990 | http://tempetes.meteo.fr/Viviane-du-26-au-28-fevrier-1990.html<br>http://tempetes.meteo.fr/Herta-le-03-fevrier-1990.html<br>http://tempetes.meteo.fr/Daria-le-25-janvier-1990.html |
| 1989 | 11,8 | Yes | Yes | 2/25/89 | http://www.meteo-paris.com/chronique/annee/1989, with<br>https://www.prevision-meteo.ch/almanach/1989 |
| 1988 | 5,9 | No | Yes | / | |
| 1987 | 11,8 | Yes | Yes | 10/15/87 | http://tempetes.meteo.fr/L-ouragan-du-15-au-16-octobre-1987.html |
| 1986 | 11,8 | Yes | Yes | 12/7/86 | http://www.meteo-paris.com/chronique/annee/1986 |
| 1985 | 5,9 | Probably | ? | 11/22/84 | http://tempetes.meteo.fr/Tempetes-du-22-au-24-novembre-1984.html |
| 1984 | 0,0 | No | Yes | / | |
| 1983 | 11,8 | Yes | Yes | 11/6/82 | http://tempetes.meteo.fr/Tempete-du-6-au-8-novembre-1982.html |
| 1982 | 0,0 | No | Yes | / | |
| 1981 | 0,0 | No | Yes | / | |
| 1980 | 0,0 | Yes | No | 12/15/79 | http://tempetes.meteo.fr/Tempete-du-15-decembre-1979.html |
| 1979 | 0,0 | No | Yes | / | |
| 1978 | 15,4 | Yes | Yes | 1/11/78 | MetMat n°101, avaiable at http://nauticalfree.free.fr/metmar/metmar1a217.html |
| 1977 | 25,0 | Yes | Yes | 12/2/76 | http://tempetes.meteo.fr/Tempete-du-2-decembre-1976.html |
| 1976 | 0,0 | No | Yes | / | |
| 1975 | 8,3 | No | Yes | / | |
| 1974 | 0,0 | Probably | ? | 2/6/74 | Archives Municipales de Nantes, 24PRES 49 du 07/02/1974 |
| 1973 | 0,0 | No | Yes | / | |
| 1972 | 9,1 | Yes | No | 2/13/72 | http://tempetes.meteo.fr/Tempete-du-13-fevrier-1972.html |
| 1971 | 0,0 | No | Yes | / | |
| 1970 | 9,1 | No | Yes | / | |
| 1969 | 0,0 | MI | Yes | 7/6/69 | http://tempetes.meteo.fr/Tempete-du-06-juillet-1969.html |
| 1968 | 0,0 | MI | Yes | 1/7/68 | http://tempetes.meteo.fr/Tempete-du-7-janvier-1968.html |
| 1967 | 10,0 | Yes | No | 3/12/67 | http://tempetes.meteofrance.fr/Tempete-du-12-mars-1967.html |
| 1966 | 14,3 | No | Yes | / | |
| 1965 | 33,3 | Several | Yes | 1/17/65<br>1/16/65<br>1/13/65 | http://www.meteo-paris.com/chronique/annee/1965, with<br>https://www.infoclimat.fr/historic-details-evenement-482-archives.html for all three events |
| 1964 | 0,0 | Probably | ? | 11/1/63 | Archives Départementales de Loire-Atlantique, PR 967 58 du 02-03/11/1963 |
| 1963 | 0,0 | No | Yes | / | |
| 1962 | 0,0 | No | Yes | / | |
| 1961 | 0,0 | No | Yes | / | |
| 1960 | 20,0 | No | Yes | / | |
| 1959 | 20,0 | No | Yes | / | |
| 1958 | 20,0 | No | Yes | / | |
| 1957 | 0,0 | No | Yes | / | |
| 1956 | 0,0 | No | Yes | / | |
| 1955 | 0,0 | No | Yes | / | |

**\* Known storm**

| | |
|---|---|
| Yes | Impacting storm(s) inventoried in the area during the studied tree year |
| Probably | Storm inventoried, probably impacting the area of our sampled forest |
| No | Any storm inventoried<br>- or MI, for Minor Impact : One or several storms inventoried with little or no impact on the studied site |

Table 2